

**PARTIAL DISCHARGE CLASSIFICATION FOR XLPE CABLE
JOINTS USING K NEAREST NEIGHBORS ALGORITHM**

MUHAMMAD SHAIRAZI BIN MOHD SALLEH

**FACULTY OF ENGINEERING
UNIVERSITY OF MALAYA
KUALA LUMPUR**

2020

**PARTIAL DISCHARGE CLASSIFICATION FOR
XLPE CABLE JOINTS USING K NEAREST
NEIGHBORS ALGORITHM**

MUHAMMAD SHAIRAZI BIN MOHD SALLEH

**DISSERTATION SUBMITTED IN FULFILMENT OF
THE REQUIREMENTS FOR THE DEGREE OF MASTER
ENGINEERING**

**FACULTY OF ENGINEERING
UNIVERSITY OF MALAYA
KUALA LUMPUR**

2020

UNIVERSITY OF MALAYA
ORIGINAL LITERARY WORK DECLARATION

Name of Candidate: Muhammad Shairazi Bin Mohd Salleh

Matric No: 17

Name of Degree: Master of Engineering

Title of Dissertation: Partial Discharge Classification For XLPE Cable Joints
Using K Nearest Neighbors Algorithm

Field of Study: High Voltage

I do solemnly and sincerely declare that:

- (1) I am the sole author/writer of this Work;
- (2) This Work is original;
- (3) Any use of any work in which copyright exists was done by way of fair dealing and for permitted purposes and any excerpt or extract from, or reference to or reproduction of any copyright work has been disclosed expressly and sufficiently and the title of the Work and its authorship have been acknowledged in this Work;
- (4) I do not have any actual knowledge nor do I ought reasonably to know that the making of this work constitutes an infringement of any copyright work;
- (5) I hereby assign all and every rights in the copyright to this Work to the University of Malaya ("UM"), who henceforth shall be owner of the copyright in this Work and that any reproduction or use in any form or by any means whatsoever is prohibited without the written consent of UM having been first had and obtained;
- (6) I am fully aware that if in the course of making this Work I have infringed any copyright whether intentionally or otherwise, I may be subject to legal action or any other action as may be determined by UM.

Candidate's Signature

Date:

Subscribed and solemnly declared before,

Witness's Signature

Date:

Name:

Designation

ABSTRACT

Due to excellent mechanical and electrical properties, cross-linked polyethylene (XLPE) cables are commonly used in the power industry. However, cable joints are the weakest part of XLPE cables and are susceptible to insulation failures. Cable joint insulation breakup can cause large losses for power companies. It is therefore necessary to evaluate the consistency of the insulation for early detection of insulation failure. It is known that there is a link between the partial discharge (PD) and the quality of the insulation. PD analysis is an important tool for assessing the quality of insulation in cable joints. In this study, XLPE cable joints with artificial defects, which are commonly found on-site, were prepared. The input data from the PD measurement results were used to train k-nearest neighbor (KNN) algorithm to classify each type of defect in the cable joint samples. Discrete wavelet transform (DWT) was used to denoise the PD signals and denoised PD signals were used to identify different types of defect in cable joints. The extracted input features from the denoised signals were used to train the classifier. Classifications were also carried out using support vector machine (SVM) and artificial neural network (ANN) for comparison with KNN. The performance of each method was evaluated through its accuracy. From the comparison of the results obtained, it was found that the approach for partial discharge of cable joint defect signals using DWT method and classified by KNN yields the highest accuracy among all of the methods tested under different signal-to-noise ratios.

Keywords: Partial Discharge Classification, Artificial Intelligence, Cable Insulation, Signal Processing Approaches, High Voltage (HV)

ABSTRAK

Oleh kerana sifat mekanikal dan elektrik yang sangat baik, kabel polietilena bersilang silang (XLPE) biasanya digunakan dalam industri tenaga. Walau bagaimanapun, sambungan kabel adalah bahagian kabel XLPE yang paling lemah dan terdedah kepada kerosakan penebat. Pecahan penebat sambungan kabel boleh menyebabkan kerugian besar bagi syarikat kuasa. Oleh itu, adalah perlu untuk menilai konsistensi penebat untuk pengesanan awal kegagalan penebat. Oleh itu, diketahui bahawa terdapat hubungan antara pelepasan separa (PD) dan kualiti penebat. Analisis PD adalah alat penting untuk menilai kualiti penebat pada sambungan kabel. Dalam kajian ini, sambungan kabel XLPE dengan kecacatan buatan, yang biasanya dijumpai di lokasi telah disediakan. Data input dari hasil pengukuran PD digunakan untuk melatih algoritma k-terdekat tetangga (KNN) untuk mengklasifikasikan setiap jenis kecacatan pada sampel sambungan kabel. Transformasi wavelet diskrit (DWT) digunakan untuk mengesahkan isyarat PD dan isyarat PD denoised digunakan untuk mengenal pasti pelbagai jenis kecacatan pada sambungan kabel. Pengekstrakan ciri data input yang diekstrak dari isyarat denoised digunakan untuk melatih pengelasan. Klasifikasi juga dilakukan menggunakan mesin vektor sokongan (SVM) dan rangkaian neural buatan (ANN) untuk perbandingan dengan KNN. Prestasi setiap kaedah dinilai melalui ketepatannya. Daripada perbandingan hasil yang diperolehi, didapati bahawa pendekatan untuk pembebasan separa isyarat kecacatan sambungan kabel menggunakan kaedah DWT dan diklasifikasikan oleh KNN menghasilkan ketepatan tertinggi di antara semua kaedah yang diuji dengan nisbah isyarat-ke-bunyi yang berbeza.

ACKNOWLEDGEMENTS

A sincere gratitude to the Almighty for blessing me a strength and a good health in completing this research work. My profound gratitude to my supervisor Associate Professor Ir. Dr. Hazlee Azil Bin Illias for his excellent supervision, guidance and continuous supports throughout my time in the university. He has provided me with useful advices, knowledge, experience and wisdom without hesitation made me able to complete this research work. Furthermore, I would like to express my deepest gratitude towards my families for their endless prayers, continuous supports and strength, which encouraged me to complete this research work. Finally, I would also like to thank to all lecturers, friends and University of Malaya (UM) for the supports and providing me the basic needed of knowledge and opportunity to learn at this institution in completing this research work.

TABLE OF CONTENTS

Abstract	iii
Abstrak	iv
Acknowledgements	v
Table of Contents	vi
List of Figures	viii
List of Tables	ix
List of Symbols and Abbreviations.....	xi
CHAPTER 1: INTRODUCTION.....	1
1.1 Introduction.....	1
1.2 Problem Statement.....	2
1.3 Objective.....	2
1.4 Dissertation Structure	3
CHAPTER 2: LITERATURE REVIEW.....	4
2.1 Introduction.....	4
2.2 Cross linked Polyethylene (XLPE) Cable Joints	4
2.3 Partial Discharge (PD).....	5
2.4 Partial Discharge Classification.....	6
2.4.1 Void Discharge	6
2.4.2 Corona Discharge	7
2.4.3 Surface Discharge.....	8
2.5 Partial Discharge Analysis.....	8
2.6 Partial Discharge Classification Features	9
2.6.1 Artificial Neural Network (ANN)	10

2.6.2 Support Vector Machine (SVM)	12
2.6.3 Convolutional Neural Network (CNN)	14
2.6.4 K Nearest Neighbor (KNN).....	17
CHAPTER 3: METHODOLOGY.....	21
3.1 Introduction.....	21
3.2 Preparation of XLPE Cable Joint Sample	23
3.3 Measurement of partial discharge.....	24
3.4 PD Signal Processing Approaches.....	27
3.4.1 Discrete Wavelet Transform (DWT).....	27
3.5 Classification of Partial Discharge	28
3.5.1 K-Nearest Neighbor (kNN)	28
3.5.3 Artificial Neural Network (ANN)	31
CHAPTER 4: DISCUSSIONS AND RESULTS	35
4.1 Introduction	35
4.2 K Nearest Neighbor (KNN).....	35
4.3 Support Vector Machine (SVM)	42
4.4 Artificial Neural Network (ANN)	48
4.5 PD Signals After DWT	55
4.6 Classification Results.....	59
CHAPTER 5: RECOMMENDATIONS AND CONCLUSIONS.....	60
5.1 Conclusions	60
5.2 Recommendations on future work.....	61
References	62

LIST OF FIGURES

Figure 2.1 Void Discharge	7
Figure 2.2 Corona Discharge	8
Figure 2.3 Surface Discharge on Dielectric Material Surface	8
Figure 3.1 Overall work methodology	22
Figure 3.2 Type of Defects	24
Figure 3.3 Design of PD measurement on AC voltage	25
Figure 3.4 Installation of HV test PD measurements.....	26
Figure 3.5 k nearest neighbor diagram.....	29
Figure 3.6 Typical neural network architecture	33
Figure 3.7 Artificial Neural Network of Feed Forward (ANN).....	34
Figure 4.1 (a) Clean PD signal and (b) noisy PD signal after DWT for defect C1 (insulation incision defect).....	55
Figure 4.2: (a) Clean PD signal and (b) noisy PD signal after DWT for defect C2 (axial path shift defect).....	56
Figure 4.3: (a) Clean PD signal and (b) noisy PD signal after DWT for defect C3 (semiconductor layer tip defect)	57
Figure 4.4: (a) Clean PD signal and (b) noisy PD signal after DWT for defect C4 (Metal particle on XLPE defect).....	58

LIST OF TABLES

Table 3.1: Defects with XLPE Cable joint Samples	23
Table 4.1: Accuracy (%) using KNN at SNR = 10 dB	36
Table 4.2: Accuracy (%) using KNN at SNR = 20 dB	36
Table 4.3: Accuracy (%) using KNN at SNR = 30 dB	37
Table 4.4: Accuracy (%) using KNN at SNR = 40 dB	37
Table 4.5: Accuracy (%) using KNN at SNR = 50 dB	38
Table 4.6: Accuracy (%) using KNN at SNR = 60 dB	39
Table 4.7: Accuracy (%) using KNN at SNR = 70 dB	39
Table 4.8: Accuracy (%) using KNN at SNR = 80 dB	40
Table 4.9: Accuracy (%) using KNN at SNR = 90 dB	40
Table 4.10: Accuracy (%) using KNN at SNR = 100 dB	41
Table 4.11: Accuracy (%) using SVM at SNR = 10 dB	42
Table 4.12: Accuracy (%) using SVM at SNR = 20 dB	43
Table 4.13: Accuracy (%) using SVM at SNR = 30 dB	43
Table 4.14: Accuracy (%) using SVM at SNR = 40 dB	44
Table 4.15: Accuracy (%) using SVM at SNR = 50 dB	44
Table 4.16: Accuracy (%) using SVM at SNR = 60 dB	45
Table 4.17: Accuracy (%) using SVM at SNR = 70 dB	46
Table 4.18: Accuracy (%) using SVM at SNR = 80 dB	46
Table 4.19: Accuracy (%) using SVM at SNR = 90 dB	47
Table 4.20: Accuracy (%) using SVM at SNR = 100 dB	47
Table 4.21: Accuracy (%) using ANN at SNR = 10 dB	48
Table 4.22: Accuracy (%) using ANN at SNR = 20 dB	49

Table 4.23: Accuracy (%) using ANN at SNR = 30 dB	49
Table 4.24: Accuracy (%) using ANN at SNR = 40 dB	50
Table 4.25: Accuracy (%) using ANN at SNR = 50 dB	51
Table 4.26: Accuracy (%) using ANN at SNR = 60 dB	51
Table 4.27: Accuracy (%) using ANN at SNR = 70 dB	52
Table 4.28: Accuracy (%) using ANN at SNR = 80 dB	52
Table 4.29: Accuracy (%) using ANN at SNR = 90 dB	53
Table 4.30: Accuracy (%) using ANN at SNR = 100 dB	54
Table 4.31: Comparison of accuracy (%) between different classifiers	59

University of Malaya

LIST OF SYMBOLS AND ABBREVIATIONS

AC	:	Alternating current
ANN	:	Artificial neural network
BPNN	:	Back propagation neural network
CNN	:	Convolutional neural network
CDBN	:	Convolutional deep belief network
db	:	Daubechies
DWT	:	Discrete wavelet transform
DC	:	Direct current
ENN	:	Ensemble neural network
GIS	:	Gas insulated switchgear
HV	:	High Voltage
IEC	:	International electrotechnical commission
IEEE	:	Institute of Electrical and Electronics Engineers
kV	:	Kilo Volt
KNN	:	K nearest neighbor
PCA	:	Principle component analysis
PD	:	Partial Discharge
PNN	:	Probabilistic neural network
PRPD	:	Phase resolved partial discharge
RBPNN	:	Radial basis probabilistic neural network
RF	:	Radio Frequency
SVM	:	Support vector machine
XLPE	:	Cross linked polyethylene

CHAPTER 1: INTRODUCTION

1.1 Introduction

Electrical insulation is an important part of all the power equipment with high voltage. Failure will be disruptive to power generation and transmission companies in any part of the power system. Hence, daily insulation quality checks are extremely important. Lifetime function of large power system equipment, such as high voltage (HV) cables transformers and gas-insulated switchgear (GIS), is highly dependent on insulation efficiency. Devices of the power system will be permanently impaired in case of a breakdown of the insulation. Some part that has failure in the power equipment will impact transmission and power generation businesses. It is therefore important that the insulation quality of power system equipment is tested and inspected periodically. Analyzing failures reveals that insulation failure is the root cause for more than half of high voltage equipment damage [1]. Cross-linked polyethylene (XLPE) has balanced electrical, mechanical and thermal materials [2] and has been widely used for HV cables insulation [3]. Cable joints are generally known as dielectrically weaknesses for XLPE cables due to the existence of discontinuity of the insulation and the manmade design of their construction [4]. PD measurement is indeed a reliable method that has been globally recognized as an important research method with the ability to evaluate and analyze insulation systems with their quality throughout manufacturing and during operation [5].

Partial discharge (PD) is a type of breakdown that does not fully connect the electrodes. This can lead to serious insulation damage and considerably reduce the life span of high voltage equipment [6]. PD occurs if the local electric field is greater than the threshold value, causing a partial breakdown of the surrounding medium [7] PD has a transient nature and is characterized by pulsating currents with a duration of several nanoseconds

to few microseconds [8]. PD is recurring in nature [9] [10] and is Capable of transmitting across dielectric material. These could severely damage the insulation and reduce the life period of the HV equipment service [6]. It is also essential to analyze cable insulation, as cable processes need to be sustained and superseded in order to avoid unexpected failures.

1.2 Problem Statement

A number of researches on the classification of cross-linked polyethylene cable joint defect types have been carried out and have improved over the years. Nevertheless, the optimal approach always needs to be achieved. There is also a need for more detailed research into how various derived partial discharge signals have an effect on the classification accuracy of the cable joint defect types.

In this research, define defect types in XLPE cable joint using k-nearest neighbor (KNN) was performed. The measurement of PD was performed on four XLPE cable joints with different artificial defects. The extraction of features from DWT signals has been used to generate data from the PD data to identify cable joints defects. Consequently, The result was evaluated between different extractions of features artificial intelligence approaches and current works.

1.3 Objective

1. To measure partial discharge (PD) through artificially designed joint defects of the cable
2. To classify partial discharge types from cross-linked polyethylene (XLPE) cable joints using k-nearest neighbor (KNN)
3. To compared of classifier performance between various artificial neural networks under different signal-to-noise ratios

1.4 Dissertation Structure

Chapter 1 describes the overview of the work 's research, problem statement and objectives. This chapter presents most of these topics. Chapter 2 concentrates with the Partial Discharge (PD) principles. This chapter includes a literature review from previous PD phenomenon relevant fieldwork. Chapter 3 deals with the methodology of study used to meet the purpose of this research work. This includes developing the cross-linked polyethylene (XLPE) cable joints, setting up the PD measurement and applying the extraction method and classification. Chapter 4 discusses all the outcomes of measurement and classification which were carried out systematically in this research. This chapter also compares data between different techniques for the classification. Finally, Chapter 5 describes the conclusions for this research and the proposed future work.

CHAPTER 2: LITERATURE REVIEW

2.1 Introduction

This chapter begins with partial discharge (PD) details, PD types and cross-linked cable joints for polyethylene (XLPE). PD measurement techniques are further explained by the fact that it's one of the diagnostic tools used to identify defects in insulating power cables in order to avoid a complete collapse of the whole high voltage power grid. It also provides a detailed overview of previous PD classification studies.

2.2 Cross linked Polyethylene (XLPE) Cable Joints

Cross linked polyethylene (XLPE) has well balanced thermal, electrical and mechanical properties and is commonly used to insulate electrical cables [3]. Cable joints are needed to connect different XLPE cables. The installation of a cable joint can be a very complicated process involving high skilled, professional cable joints.

In the power industry there are two different types of cable joints used in the heat shrink tube and cold-shrink tube cable joints. The termination of heat-shrink requires multiple instruments, including gas torches and flame retardants. Cold-shrink and heat-shrink termination cables require a wide range of measurement methods. Heat-shrink needs very detailed ability since inaccurate shrinkage will lead to incomplete installation. Overheating would cause scorch and malfunction to the XLPE cable while heat shrinkage.

Cold shrinking cable joints need no heat source and are more robust and less prone to technical mistake. Installation is also better without additional equipment and training. Once the support core is removed, the cold-shrink tube shrinks and forms a cable joint between the two XLPE ends. As the cold-shrink tube goes through thermal extensions and shrinkage, it is more versatile than the hot-shrink tube.

By linking all high voltage cables, two main measures must be taken. The conductive covering on the exterior side between both cables must then be immediately terminated and without creating ground concentration. It is suitable for the design of the cable terminals. Secondly, a loss of flexibility or resources between the cable displacement area as well as the cable conductors is prevented [11].

2.3 Partial Discharge (PD)

Early detection and diagnosis of high voltage (HV) equipment is necessary to ensure the performance of the entire power system, especially for the diagnosis of voltage sag [12]. Partial discharge (PD) could be root cause of a sudden failure that impacts the insulation leading to a surface charge of the insulation, contributing to chemical and physical degradation and might cause an unpredictable breakdown [13]. Partial Discharge (PD) is an electrical discharge that happens when the HV components is normally protected due to the presence of cavities or contaminants, resulting in production process failure mechanical stress or aging process [9]. Therefore it is important to monitor the insulation that has been used in HV system so that preventive actions can be conducted at the right time [14].

Damage to power cables is commonly attributed to mining activities [15]. Furthermore, the severe damage to the network cable electrical insulation causes damage to even more than quarter of the cable network. The AC and DC analysis is a study approach which has only been used for the power cable network for many years, but today the PD test is also a widely accepted method. Partial Discharge (PD) is one of the most important causes of deterioration of cable insulation process or training. Partial Discharge (PD) deteriorates the insulation and therefore can cause loss of energy.

The cables and adapters establish good connections and terminations within the actual power cable network. The main function of a joints is to link both cables to each other while positioning the end point of the cable. PD faults usually occur in cable joints and

cable terminations themselves, as they are constantly built under imperfect conditions [16]. The XLPE cable joint loss rate is higher than a cable in the power systems leading to inadequate environmental conditions, inconsistent installation and degradation [17]. Throughout the installation of cable components, there are many factors to consider to avoid deterioration of the insulation. Demolishing cable joints needs a professional cable joints expert since this is an extremely complicated task.

2.4 Partial Discharge Classification

The thermal substances of the networks take many forms of gaseous, liquid or solid and it is understood that the high voltage (HV) network does not have full insulation. The impurities or pollutants thus gives the possibility of partial discharge (PD) and impacts the quality of an insulation. The insulation deteriorates and radiates outward to sustain PD phenomena. Deterioration affects the properties of the insulation due to electrical, mechanical and thermal stress. In HV technology, various forms of PD are present, such as surface, internal, and corona discharges. According to the [18] [19], internal or void discharge is severe and more volatile than surface discharge and corona discharge.

2.4.1 Void Discharge

Void discharge happens when the closed amount in the insulation substance, including such liquid and solid, is insufficient. Common types of the faults contain void, gap or corrosion, particles or cracking. A certain partial discharge (PD) are normally caused by the production process or by power cable attachments along with other joints or terminations.

The electrical current on the surface insulation is smaller than electrical field within the void throughout this element of PD. The nature of the defect transitions from non-conducting to operating during a PD event, resulting in a reduction of the applied voltage and within enclosure from higher to smaller during a very short time.

These allows its insulation quality to become corrosive as PD behaviors are performed over time, leading to a failure. Void Discharge is show in Figure 2.1

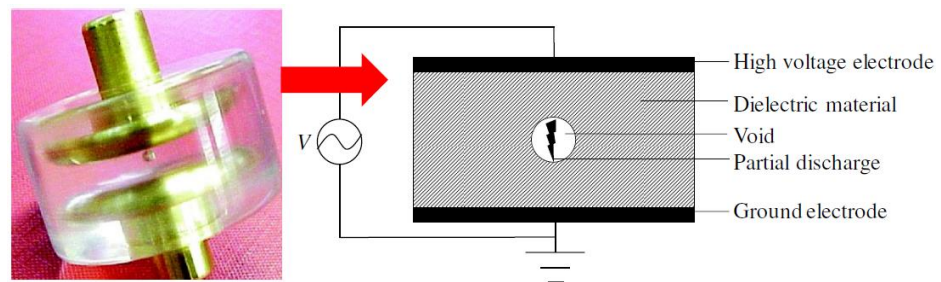


Figure 2.1 Void Discharge

2.4.2 Corona Discharge

Corona discharge is also identified as a moving discharge once the ionization from the air in the outer conductor boosts to a certain vital value due to an electric field [20]. It will occur if the electric field at a sharp-points exceeds the air degradation level. There will be two different types, positive and negative, of the corona. Corona 's consequences are voltage drop in the power grid due to current flows off the current path, noise pollution, radio interference and separation depletion. This is not normally described to be a volatile discharge, but corona process is the same as other kinds in PD and may seem a violation of online measurement [13]. Corona Discharge is shown in Figure 2.2.

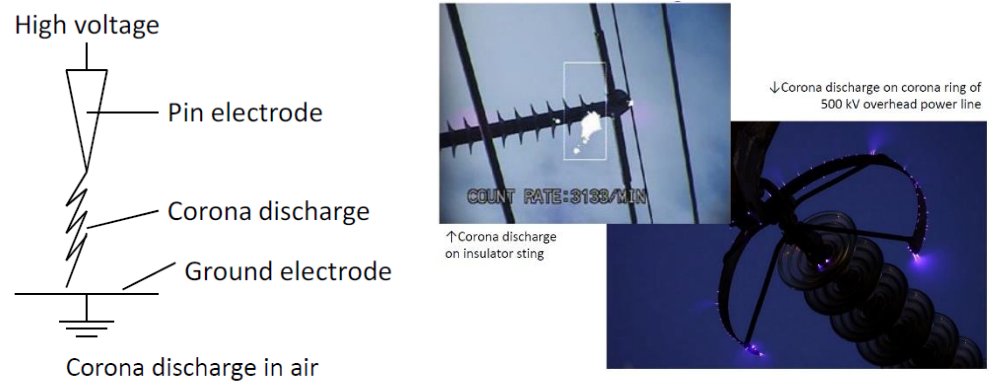


Figure 2.2 Corona Discharge

2.4.3 Surface Discharge

Discharge happening upon a surface of the thermal insulation particles is considered surface discharge, at which tangent surface area is high. This discharge bridges the difference in the source potential and the earth electrode through radiation exposure or leaks on the insulation sheet. The highest level isolation on HV cables or the end of the sizeable generator stator windings are instances of surface discharge in this field. Surface discharge is shown in Figure 2.3.

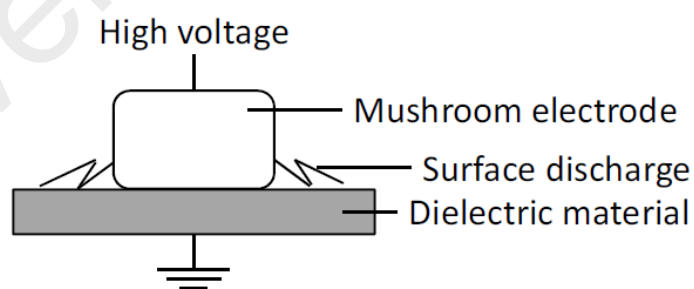


Figure 2.3 Surface Discharge on Dielectric Material Surface

2.5 Partial Discharge Analysis

High voltage or current pulse applications are based on modern PD fault detection. The commercially available electrical pulse detection device can be used in high voltage

(HV) research facilities [21]. Pulse detection systems have their own benefits and drawbacks [22]. This approach benefits from high demand for businesses, the ability to identify PD values, automated measurement assisted by the use of two sensors, the ability to interpret the PD route for cable suppliers and the ability to utilize with PD location systems. Furthermore, the drawbacks of this approach are difficult measuring equipment and challenging to implement in the field, susceptibility to radio frequency (RF) noise in the absence of shielding, weaknesses of inductive construction and restricted coupling strength reduce the responsiveness of the capacitive system.

Instrument technique uses acoustic devices to calibrate sound waves on the insulation surface. It is an important PD detection extraction method [22]. A benefits of this technique include electromagnetic protection against noise, nondestructive and nonintrusive, higher precision sensors, high frequency spectrum, no shielding design strong mechanical power high electrical conductivity resistance and more better than other sensors. Nevertheless, the drawbacks of these approach are the signals amplification, the temperature sensitivity of measurements is impaired, the PD level cannot be measured, the need for highly technical calibration and the limited ability to handle air insulation equipment [22] [23] [24] [25]. Electric pulse detector would still be a popular PD calculation method in industry. In this work the electrical pulse detector is used when it complies with the PD measuring method of IEC60270.

2.6 Partial Discharge Classification Features

Numerous studies related to a classification of partial discharge (PD) have been carried out previously. There are several classifiers analyzed in this section are Artificial Neural Network (ANN), Support Vector Machine (SVM), Convolutional Neural Network (CNN) and K-Nearest Neighbor (KNN).

2.6.1 Artificial Neural Network (ANN)

Classification of previous work partial discharge (PD) was published in [26]. The researchers studied PD pattern recognition in 66 kV cross linked polyethylene (XLPE) cables and analyzed 38 kV AC through three layers of feed back propagation neural network (NN). A neural network has three output data "no PD" for a stable PD level, "alert" for a low PD level and "alarm" for a high PD level. Phase angle voltage, pulse count and discharge amplitude were the input data for the NN. A neural network had been trained utilizing 30 input data, achieving a classification precision of 90%.

The artificial neural network (ANN) has been studied [27] for the identification of PD process. The artificial defect was artificial to surface discharge, particle progression to the oil discharge, multipoint plane discharges in oil with gas bubbles, multipoint discharges in oil, point to plane discharges in oil and point to point discharges in oil with gas bubbles, and multipoint plane discharges into oil. The method of power spectrum distribution and the fourier transform have been used as input characteristics. Greater than 90% of the classification accuracy was achieved.

PD behaviors determined from lab - based computational PD sources have been used to classify probabilistic neural network (PNN) [16]. Each input properties used were wavelet transform derived on different scales through wavelet packet conversion. The quality ratings for corona in liquid, surface air discharge, internal oil discharge and floating oil discharge is 97.5%, 92%, 100% and 99%.

The Radial Basis Probabilistic Neural Network (RBPNN) had been used in [28] to classify four kinds of partial discharge causes: corona oil, corona air, void and internal corona air. The functionality extraction were used in forward less square orthogonal. With RBPNN classification performance somewhere around 80% and

90%, PNN classification performance between 50 and 70% was achieved. Subsequently, the robust heteroscedastic probabilistic neural network (RHPNN) [28] were utilized to achieve classification accuracy of more than 90%.

ANN was used in the proposed fractal function [29] for PD recognition pattern. Deficiency classifications were established for cross linked polyethylene (XLPE) cable joints, which included a healthy power cable, a long outer semiconductor layer, an artificial knife defect and a short outer semiconductor layer in XLPE insulation. The extension method achieved 81.7% of the accuracy rate and the BPNN method achieved 73.3% of the accuracy rate when 15% of the noise was added. Features of related inputs and classification techniques were used to determine the types of high voltage transformer defects in [29].

The RF antenna [30] was used to define PD to the thermal insulation polymer under various conditions. Four cases including the active corona, inactive corona, the surface discharge and the composite PD were examined. Frequency and statistical analysis attributes were used in the classification has been done using the artificial neural network (ANN). It is suggested approach was to successfully identify PD types with more than 96% accuracy of classification.

As reported a redesign of artificial neural network known as ensemble neural network (ENN) for partial discharge (PD) performance patterns in [31]. A total of six partial discharge (PD) defects was developed at the research lab, that involves corona in oil, air surfaces, electromechanical constrained void or gap, air corona, polyethylene terephthalate (PET) single vortex and oil surface discharges. Frequent patterns were used as input and a precision classification of 95% was achieved.

In [32], using an ultra high frequency (UHF) PD to test sensor. PD signals is opposed by wavelet transform. Three kinds of PD patterns have been evaluated for deficiencies produced in laboratory conditions such as void moving metal, pressure and liquid metal. Features extracted and wavelet transform were used as input specifications for the ANN classifier and the precision of the classification obtained was 95% when denoising was used and 75% without denoising.

A phase resolved hybrid of PD data and moment resolved PD data [33] was developed to be used as an input features. A Dempster Shafer Proof Theory was used as the technique of data fusion. The following flaws, protrusion, degradation of the air, separator and free particles were used to create a GIS test sample. The classification of ANN was used as 82.94% for timeframe resolved PD data, 92% for the use of PD data resolved by process, and 97.25% in the use of fused data.

The HV equipment was used to determine PD source in Artificial Neural Network (ANN) [34]. The ANN classification was based on nine waveform parameters for each PD case. The lab developed waveform parameters for four forms of artificial PD sources and three kinds of noise sources through three different types of sensors and about 90% of the results shows accuracy precision.

2.6.2 Support Vector Machine (SVM)

A support vector machine (SVM) has been used to study the performance of partial discharge (PD) sources depending on different features [35]. Methods of extraction used included wavelet decomposition, frequency spectrum, and phase - based detail. The PD sources producing PD signal types include internal discharge, surface discharge, and corona discharge. As a PD performance investigation study, a transformer bushing device has been used. The total accuracy shows a high accuracy of 98% for the limited frequency feature.

The PD classification is performed on a support vector machine (SVM) [36]. Cylindrical glass samples were collected using two parallel flat aluminum electrodes, and four PD designs. Input functions were used as increased order moments and entropy of the measured probability density. Diverse moments mixture was measured and 98% of the best grade accuracy was achieved with six times as results.

A support vector machine (SVM) has been used in [37] to characterize PD behavior acquired from surface, corona and internal discharges. The functions of the input were extracted using the analog time frequency approach from the pulse wave. DC voltage was used to evaluate PD rather than AC voltage. The classification accuracy had never been specified, but various PD patterns were distinguished by the proposed method.

SVM was used in [38] categorize PD behaviors for artificial defects, including corona discharge, surface discharge and internal discharge. As input function the average stage charge has been used. Only two out of sixty samples had been misclassified.

A three-phase paper insulated lead (PILC) distribution cable experiment was investigated by [4] for the investigation of partial discharge (PD) of various faults. The three separate cable joint faults, including the ferrule bolt, void of the crutch and bottom, were examined. The input values used were statistical features mixed with the extracted features during the wavelet transformation. Classification performance was at 91%.

A gas insulated switchgear (GIS) simulator [39] was developed in the research lab. Four common defects in isolation, gas hole, free moving object, metal needles and fixed metal particles are popular. The input properties were a combination of

statistical factors that interact taken from chaotic theory. The SVM has been used and the detection rate of 98% is obtained.

A research on the behaviors of a gas insulated substation calculated partial discharge can be discovered in [40]. A data obtained at various SF₆ gas volumes with a particle size and position were classified by a support vector machine. The statistical input feature has been used and 94% of the accuracy rate has been achieved.

The support vector machine has been classified as a gas insulated substation on partial discharge pattern [41]. The PD forms in four groups which include an internal, corona, particles and surface discharges. Analytical techniques are used as a method of extraction and have more than 90% classification accuracy.

2.6.3 Convolutional Neural Network (CNN)

Partial discharge patterns recognition with deep convolutional neural networks proposed in [42]. The traditional pattern recognition methods of partial discharge also depend on much prior knowledge of the PD device and signal processing techniques to create suitable features. The output is therefore was not constant. Recent advances in deep neural networks, including more than one hidden layer, have shown a success in the recognition of speech, imaging and natural language processing. Deep neural networks are able to manage large data sets, a potential overall strategy because the processing of data accumulates increasingly. A deep-architected Convolutional Neural Network (CNN) has been developed formed automatically generalize innovative features to recognize ultra UHF GIS detection signals. The symmetrical signal frame classification of UHF measurements is derived by Fourier transform data collection. The spectral frames are then used to deeply

train the CNN. It was shown that the implemented method can significantly develop various PD forms.

A novel approach of Transient Earth Voltage Detection (TEV) is presented for the convolutional neural network (CNN) [43] where it does not need a signal system prepared by humans and overcomes the detection problems caused by an incorrectly extracted features. The CNN model is intended to train and interpret the TEV signal perspective. Since its proposed process does not employ a sophisticated denotation method, it is based on an exceptional detection output that shows the effectiveness of the proposed technique of CNN based TEV detection. The TEV standard and GIS methods typically consist of four stages, i.e. data collection, filtering, extraction and pattern recognition. These methods produce functionality using statistical analysis or pulse waveform analysis, and then conduct recognition and extraction of features functions. Deep learning methods are developing rapidly and have a significant impact on pattern recognition, because of their excellent recognition and extraction capabilities that significantly compensate for the low recognition performance of standard TEV methods.

In [44], the PD detection is critical in order to detect faults in high voltage cable systems. A new approach used to identify PD pictures based on the Convolutional Deep Belief Network (CDBN) was introduced to increase the accuracy of the DC cross linked polyethylene (XLPE) insulation fault classification. Four cable defect forms XLPE was developed and tested with DC voltage. The image $q - \Delta t - n$ is built on the basis of the PD measurements received by HFCT. The CDBN-diagnostic model is then constructed for high level detailed $q - \Delta t - n$ images with Gaussian visible devices. Finally, there is the testing of CDBN classification, Deep Belief Network (DBN), SVM and BPNN. The experimental

results show approach is more effective in diagnosing the isolation defect with an accuracy of 93.8%.

A DC XLPE cables based on convolutional neural network partial discharge pattern recognition is proposed in [45]. A self adapting pattern recognition method based on a convolutional neural network (CNN) is used to overcome the drawbacks of high random signal extraction feature in DC XLPE cables. CNN has a strong performance in image recognition, with convolutional architecture fast feature embedding (Caffe). There are four common insulation defects and PD signals for pattern recognition have been developed. The presence of network structure and optimization parameters on a training effect are examined in four distinct Caffe approaches. The modified Alexnet network can be used to determine patterns of partial discharges in DC XLPE cables as compared to Quick-CIFAR-10 and the original Alexnet network, with an accuracy of 91%.

A differential partial discharge (PD) induced by different types of insulation defects in high voltage cables was used in [46] and known as convolutional neural network based deep learning methodology for recognition of high voltage partial discharge patterns. Most PD signals have quite comparable characteristics and are especially difficult to differentiate, even the most experienced engineers. A PD test is performed in a high voltage research lab for five forms of artificial defects on ethylene propylene rubbers to generate signals containing pd results. Then are collected 3500 transient PD pulses, followed by 33 PD classifications. The next step applies CNN to the results, defining the typical CNN architecture and the key factors affecting the accuracy of CNN pattern recognition. The discussed considerations include number of network layers, complex kernel size, activation mechanism, and the pooling process. It provides an overview of 3500 sets of PD samples, the CNN

based PD pattern recognition system. The performance of a CNN based architecture identification are 92.57% and two other traditional methods, i.e. 87.81% support vector machine (SVM) and 86.10% back propagation neural network (BPNN) have been contrasted to the proposed approach. A results showed that the proposed CNN method is more accurate than the SVM and BPNN methods for pattern recognition and that the new method is particularly effective in the case of highly similar signals relevant to industrial applications for PD form recognition.

2.6.4 K Nearest Neighbor (KNN)

Effective disturbance extraction is important for the safety and stability of the power system. In [47], the proposed new detection method is based on the k nearest Neighbor (KNN) application of the time series analysis methodology. The benefits of this method are that electrical calculations can be controlled using oscillations patterns and implemented in real times. The technique comprises two phases: off-line and on-line detection. The offline process calculates the anomaly index series using kNN on the historical environmental data, and decides then the threshold for identification. The online stage then determines the anomaly index value of the currently measured data by readopting kNN and compares it to the threshold set to intercept disturbances. In order to meet the real - time specification, strategies are developed to recurrently measure kNN distance metrics and to automatically pick the smallest kth metric. Research studies carried out on simulation data from the Great Britain power system's reduced equivalent model and observations from an actual power system in Europe indicate the effectiveness of the proposed technique.

K - nearest neighbor rule (KNN) and sparse representation (SR) algorithms are widely used in pattern recognition. In [48], two new neighbor classification methods are proposed in which the existing weighted voting methods are established

to render classification decisions on the basis of low SR coefficients. Since the sparse coefficients can represent the neighborhood structure of data, we assumption them to build classifier in the proposed techniques. One alternative method is called the coefficient weighted KNN classifier, which implements sparse coefficients for selecting KNNs from a query sample and then uses the coefficients corresponding to the neighbors selected as their classification values. The residual-weighted KNN classifier (RWKNN) is another new approach. In the RWKNN, the KNNs of a query sample are first defined by low coefficients and then a modern residual based weighted voting process is built for the KNN classification. The comprehensive studies are done on several UCI and KEEL sets of data, and the simulation results reveal that the methods proposed are running well.

In [49] present a k - nearest neighbor (k - NN) approach to estimate defect locations for all forms of parallel fault lines utilizing single-terminal standard measure. Discrete Fourier Transform (DFT) is being used to preprocess signals and then the standard deviation of one pre-fault phase and one post-fault measurement cycle are used as inputs to the kNN algorithm. The obtained results through specific fault conditions show the significant accuracy of proposed scheme for estimating the fault positions. The specificity of the k - NN fault location scheme is not affected by changes in the fault type, including inter circuit faults, fault location, fault level, fault resistance and angle of load pre-fault.

In [50], The research proposed a distributed storage and computation algorithm (D-kNN). The following advantages refer to the D-kNN algorithm. A classic supervised machine learning algorithm, the K nearest neighbor (kNN) algorithm is. It's commonly used for data collection and processing in cyber physical social systems (CPSS). In practical CPSS implementations, the regular linear kNN

algorithm fails to efficiently process massive data sets. Next, the definition of the k -nearest neighbor boundary is introduced and the k nearest neighbor check within the k nearest neighbors boundary will essentially reduce time complexity of the k NN. Furthermore, based on the k -neighbor cap, massive data sets are placed on distributed storage nodes beyond the central data storage. Consequently, the algorithm performs effective searches of k nearest neighbor by running distributed calculations at each storage nodes. Eventually, a series of experiments were carried out to check the efficiency of the D - k NN algorithm. The test results reveal that the D - k NN algorithm, based on distributed storage and computation, effectively improves the operating efficiency of the k nearest neighbor search. The algorithm can be deployed easily and flexibly in a cloud based computer environment to process massive data sets within CPSS.

Industrial collected data have highly nonlinear or multidisciplinary qualities which do not comply with statistical data assumptions in the principal component analysis (PCA). PCA thus has a lower rate of detection of faults in process industries. Purpose of the above limitations of the PCA, In [51] mentioned a fault detection in the Tennessee Eastman Benchmark using principal component difference based on k -nearest neighbors (Diff-PCA). Initially, and each sample's nearest k neighbors set in the training data set and determine its mean vector. Second, use every sample and its corresponding mean vector to construct an augmented vector. Thirdly, using PCA to measure the load matrix and performance matrix. Then, calculate the overall scores using each sample's mean vector and the required PCA data imputation technique. Finally, create two new numbers, using the difference between the actual scores and the predicted scores to detect errors. In addition, this paper also proposes the fault diagnostic method based on contribution plots of monitored variables. Throughout Diff-PCA, the ability of difference will remove the effect of the

nonlinear and multidimensional system on detection of faults. In the meantime, the subspaces monitored by the two new statistics differ from that of T^2 in PCA, and SPE. Throughout two numerical cases (nonlinear and multimode) and in the Tennessee Eastman (TE) processes, the effectiveness of the proposed strategy is implemented. The tests of fault location reveal that Diff-PCA exceeds standard PCA, kernel PCA, dynamic PCA, key component based k nearest neighbor rule and k nearest neighbor principle.

University of Malaya

CHAPTER 3: METHODOLOGY

3.1 Introduction

This chapter sets out the framework for the planning phase involved in the design of this project. This contains an overview of the project from start to finish. Cable joint samples, described in detail for PD planning, PD measurement setup and PD classification. It also explains and illustrates the methods used to achieve this project. The training process has been repeated until good accuracy has been achieved. This section is meant to ensure that a project objectives are done to achieve.

PD experiment were conducted in a HV enclosure cage to prevent some mistake occurring throughout the experimentation. The PD flowchart used in this study is shown in Figure 3.1. XLPE defect cable joint samples were planned and PD analyses were carried out. Component extraction is utilized to determine input features that is used as data input for classifiers. This same process is then repeated again until most excellent performance had been found. The experiment was conducted within below 9 kV of voltage. The PD calculation results are achieved by means of cable energy at less than 9 kV. A total of 100 signals have been conducted for each sample at a range of 60 seconds. As for the four XLPE cable joints samples a total PD of 400 signals was therefore obtained.

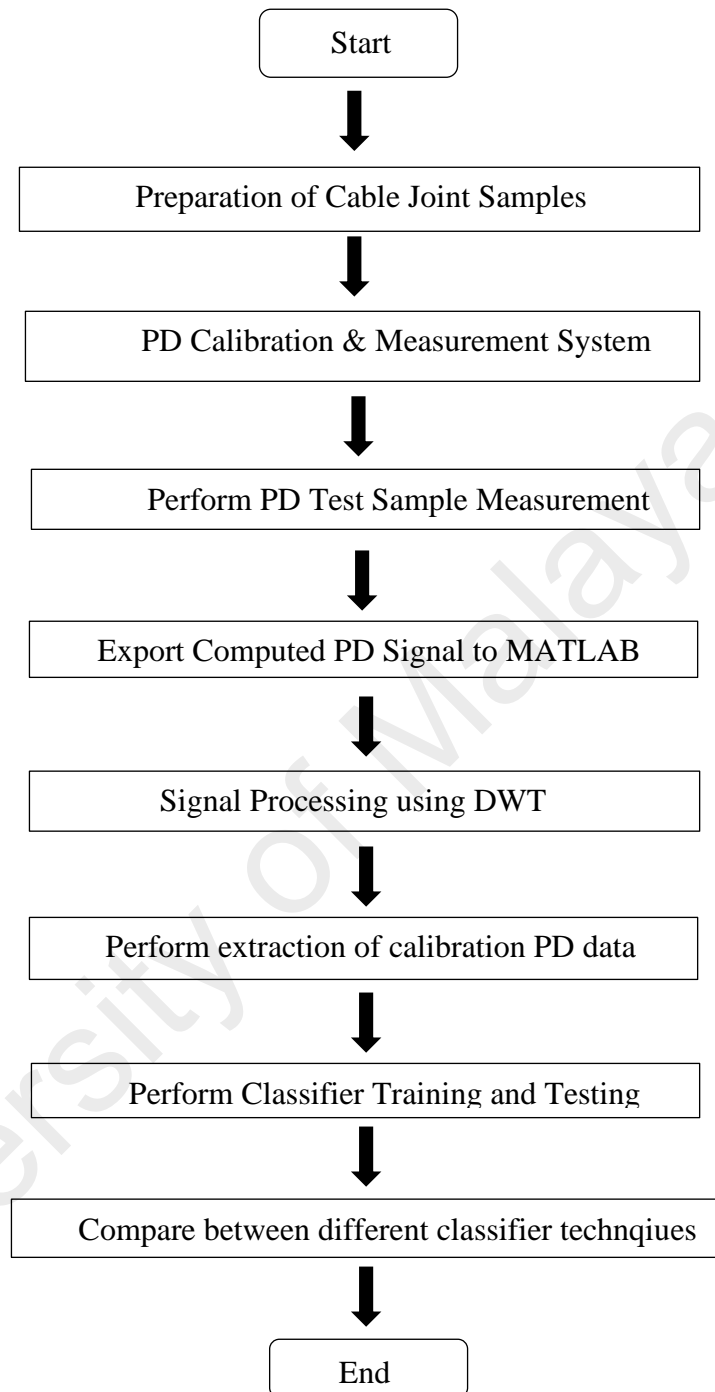


Figure 3.1 Overall work methodology

3.2 Preparation of XLPE Cable Joint Sample

A four XLPE 11kV cable joints with developing various defects has been used in this research. From each sample, a cable length of 3 meters with a cable joint located in the centre was used. The XLPE cable joint sample lists are shown in Table 3.1.

Table 3.1: Defects with XLPE Cable joint Samples

Joint Cable	Type of Defect
C1	Insulation incision defect
C2	Axial direction shift defect
C3	Semiconductor layer tip defect
C4	Metal particle on XLPE defect

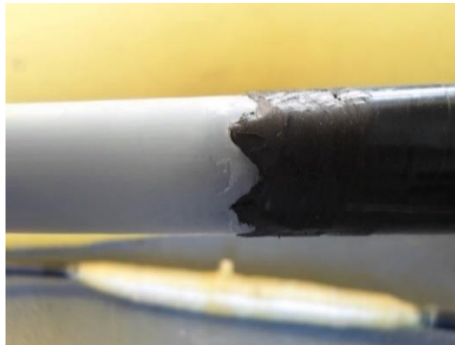
The incision insulation was caused by a shallow cut of the XLPE layer with a sharp knife. Impact on the axis of change was induced by using the angle of the cables from an off centre. Through creating a rough edge in the semiconductor the tip defect in the semiconductor layer is presented. The sprinkling metal particles on the XLPE layer formed metal particles on the XLPE fault. All faults were rendered in the construction of XLPE cable joint. The cable defect image is shown in Figure 3.2.



(a) **Insulation incision defect**



(b) **Axial direct shift defect**



(c) Semiconductor layer tip defect



(d) Metal particle on XLPE defect

Figure 3.2 Type of Defects

3.3 Measurement of partial discharge

A Figure 3.3 shows a schematic diagram of the PD measurement system under AC voltage, and the actual measuring configuration in the HV laboratory is shown in Figure 3.4. A measurement system includes a step up transformer, the HV source, the testing capacitor used to determine the operating voltage, the test components, the coupling condenser, the coupling panel, the PD detector and the PC-connected USB controller. The connecting device changes the voltage current. The PC was used to customize the PD detector settings and to store data. In this study, the Omicron released the Mtronix MPD600 was used for PD measurement.

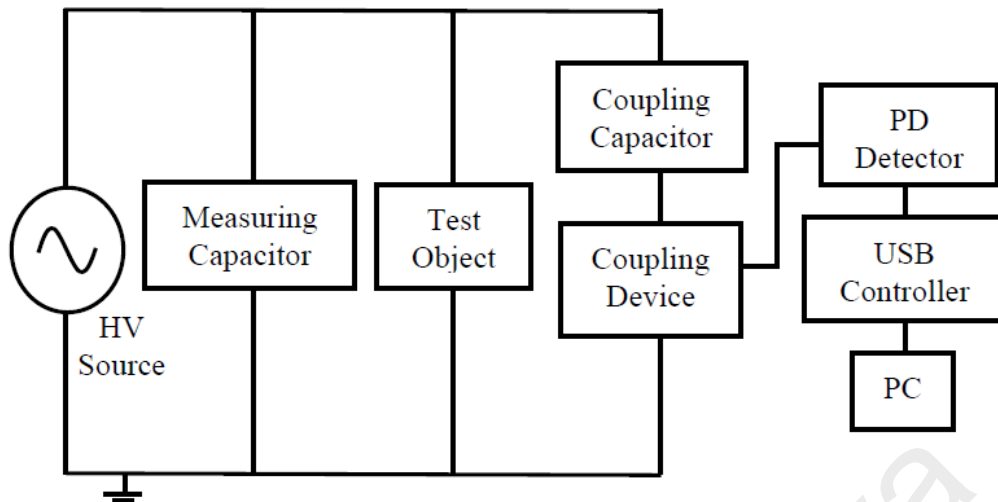


Figure 3.3 Design of PD measurement on AC voltage

It has an operating frequency ranging from 0.1 Hz to 2.5 Hz. This allows identification of a PD signal from 0 to 32 MHz, with a range of less than 2ns in the middle. This function is very precise pulse identification. The Mtronix MPD 600 system is an excellent computer system for both site and laboratory PD measurement.

Through measuring the current pulse increase between the two terminals of the test instrument, the MPD 600 analyses PD. In a test object, the coupling condenser transmits the loads to the test object to offset the voltage drop across the test object. It allows the circuit to travel through a current pulsation within the nanosecond scale, which generates a voltage pulse by the connector. This is the apparent charge, the cumulative number of payments exchanged. The total number of induced dipole moments of the actual load caused by the sudden change in the capacitance of the test subject and its interaction with the unit electrodes decide the magnitude [52]. In the case of PD, the measurement impedance or the linking tool senses a short term strain pulse.

The USB controller manages data transfer among the PC and the PD detection system. A PD detection system transmits the effects of the standard measure to the USB controller through fiber optics. Implementing fiber optic cables delivers galvanic

insulation in between USB controller and the PD detector. Apart from moment of inertia reduces interference and improves the signal to noise ratio, thus improving system performance. After the USB control receives the data , the data is transmitted via a USB cable to the laptop. The consumer can then optimize and store the simulation results.

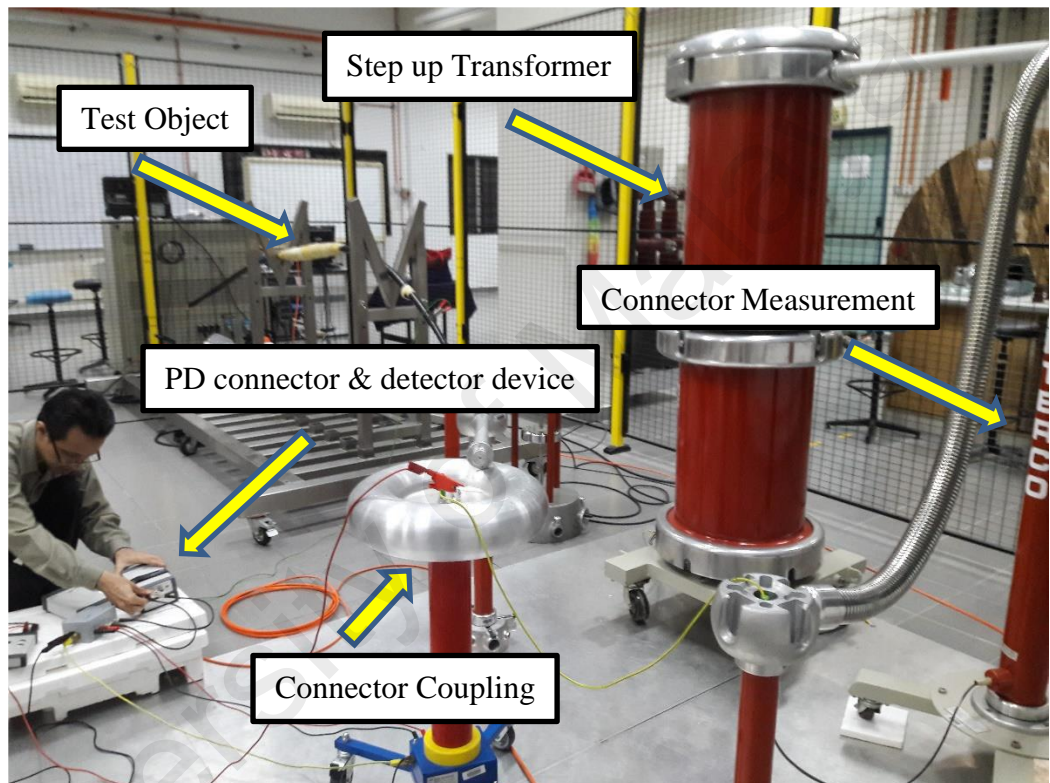


Figure 3.4 Installation of HV test PD measurements

The HV supply was attached to the test object for each PD type. Each defect was tested with a certain voltage from the source (6kV, 7kV, 9kV and 11kV). Thus every defects was therefore tested triple time to achieve a PD behaviour. The step up transformer coupling condenser connector PD detector and coupling device was mounted on the computer and the PD signals were transmitted to the PD detector from the test device.

The rise time of the signal was extracted from the obtained PD signals after discrete wavelet transform (DWT). This feature has been used as the input data for the k

nearest neighbor (KNN), artificial neural network (ANN) and the support vector machine (SVM) to classify the defect types. To order to identify the best approach for the highest classification percentage precision, the outcomes of each procedure are contrasted.

3.4 PD Signal Processing Approaches

Current data will then be analysed using signal processing software to optimize the PD classification data. In order to remove noise and vibration, the signal processing attempts. This project uses the Signal Processing software to refine the Partial Discharge Classification (PD) analysis, and to analyse raw PD signal processing. This project processes raw PD signals using a multi-signal processing technique, which is DWT.

3.4.1 Discrete Wavelet Transform (DWT)

The DWT can provide data in both time and frequency domains. A Fourier transform use a wavelet transform, which can provide feedback on frequency and time. Wavelet analysis is similar to the Fourier analysis, which breaks down the signal into its component parts for investigation. The main issue is, the consequence frame resolution length limits the frequency. A wavelet transform is infrequently and efficiently designed so that the wavelet is a good method for examining a non stationary wavelet signal. Its irregular shape can indicate discontinuity or sudden shift. With their compact support characters, a temporary localization of the signal features can be allowed.

Throughout every point of the wavelet transform, the discrete wavelet process includes a number of low pass and high pass filters. It can be considered as backpropagation of the same function, which provide accumulative details on one scale each approximation. At the end of the frequency range, the first stage will cover a broad frequency range and higher stages would hit the lower end of the frequency range with ever narrower bandwidths. The first measure

has the largest timestamp resolution and the lowest frequency resolution, whereas the other scales span longer intervals and smaller frequency bands.

The discrete wavelet transform for signal x is measured through a series of filters. This research has utilized a discrete wavelet transform (DWT), a tool for de noising a signal. [53]. It shall be specified where the discrete signal is $\varphi(n)$, whereas j and k are integers,

$$W_{j,k} = \sum_{n \in \mathbb{Z}} \varphi(n) 2^{\frac{j}{2}} \psi(2^{-j}n - k) \quad (3.1)$$

Over hundred data signals for approximation and detailed coefficients, every defect shape was determined and extracted. The signal was deliberately noised. The signals collected were subsequently trained and tested again by KNN, SVM and ANN

3.5 Classification of Partial Discharge

3.5.1 K-Nearest Neighbor (kNN)

K-nearest neighbor (kNN) [54] is a learning system based on instances or an algorithm that deferred all calculations to be easy to learn until classifying. The kNN algorithm concept is that if the sample has k most similar neighbors (i.e. the closest neighbors in the region of the characteristics) the significant number of samples belong to a certain category, then the sample is also in that classification. The voting method will usually be used in the classification process, i.e. the group mark that occurs most in the k samples is used as the prediction object, Figure 3.5 indicates the nearest k nearest neighbor diagram, so the value k is specific and the samples are viewed differently.

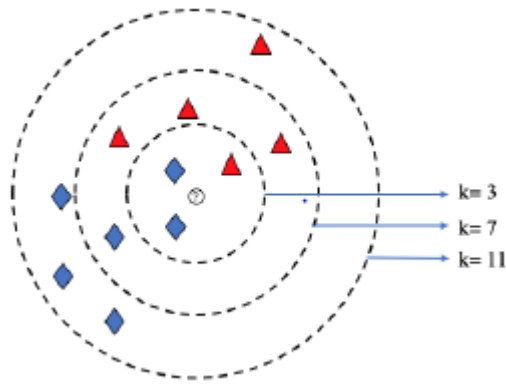


Figure 3.5 k nearest neighbor diagram

In the regression function, the average method can be used, i.e. the average actual value of the survey outcome marks can be used as a projective measure, weighted average or weighted votes can be carried out also based on the distance of the closer sample.

The schematic of the next k nearest neighbors in which k is an important parameter is shown in Figure 3.5. When k takes different values, the classification results are substantially different. The result of the sample decision is prismatic as illustrated in Figure 3.5. It is when k= 7 is a triangle, and when k= 11 is a prism of the results of the evaluation of the sample. The closest neighbors can be found significantly different when different distance methods are employed, which also results in a significantly different classification results. The closest k nearest neighbors may be located, given the distance calculation is accurate.

Theoretical basis of the KNN classic is the closest nearest neighbor rule (NNR). [54]. Let x be the marking point and the point closest to x be y in the case of an example. A potential error that occur if y is given the same label as x, as seen in Equation (3.2),

$$P^* \leq P \leq P^* \left(2 - \frac{c}{c-1} P^* \right) \quad (3.2)$$

where P^* is the Bayes error rate, c is the number of classes, and P is the error rate of the nearest neighbor. The error rate of the closest neighbor is less than half the error rate of Bayes. Since the average task failure is small, the loss is twice small. If the data center number is very growing, the probability for x and y to be similar is very small. The next neighbor algorithm from equation is relatively simple, but does not surpass the Bayesian Optimal Classifier's error rate twice which can be referred to equation (3.2).

3.5.2 Support Vector Machine (SVM)

A SVM were first invented as an application principle by V. N. Vapnik [38] capable of solving complex pattern classification problems. SVM is an algorithm of machine learning, which is based on the theory of statistical learning that can handle complex classification tasks. By using kernel methods, the SVM can be modified in different fields and tasks depending on the base algorithm and the kernel function classification. SVM is suitable for small sample size, high dimensionality and nonlinear difficulties with pattern recognition [38]. SVM transfers data to a higher dimension field through linear classification [9].

The SVM consists of a number of different principles, including linear learning machines, kernel functions, room functions, enhancement and numerical analysis. These concepts are implemented into the SVM method of training. SVM has been shown to exceed the learning algorithm in a wide range of areas [38]. SVM could be used to classify roles from the labeled training data collection. Every test data could be expressed

with a variable where its concept depends on a number of behaviors been using. its role is either divergence or preprocessing [38]. SVM has less parameters to modify, making it less dependent on empirical procedures [9].

The initial purpose of SVM was to deal with linear cases separating them. Not all practical matters, apparently are linearly separated. The standard SVM as a linear classifier are not functions in non-linear situations. A technology called a kernel to handle nonlinear problems with multiple linear classification was introduced to overcome this problem. Thus according pattern recognition principle, a smaller dimensional space and the inseparable non - linear form are transformed into a linear model by transforming this into a larger dimension. The use of the kernel form therefore prevents the measurement affliction [55].

Initially, The binary classification algorithm for SVM has been built to identify the input in only two groups [56]. Due to the fact that support vector machine utilises a hyperplane to separate data into two groups. In MATLAB you can do binary classifications using the commands "svmtrain" and "svmclassify." Multi level SVMs are needed if more than two classification classes are required [57] [58]. SVM is a multi level which carries out multiple SVMs. A sample group is listed as one class during multi-level SVM preparation, while the remaining samples as other classes.

3.5.3 Artificial Neural Network (ANN)

As PD classification is unresponsive to minimal changes in data, ANN is feasible. If its input varies significantly from the feedback used

during the workout, ANN will make the correct decisions. Regarding PD classification, this is very important where the release patterns are generally different [59]. Artificial Neural Network (ANN) has strong generalization, stability, and versatility [60] for partial discharge (PD) classification. The ANN model, such as the transfer function, and the training algorithm are defined with in network architecture.

The neural network includes several computing layers with parallel basic elements modern deep learning nervous systems. An interface layer contains one or more input and output layer respectively. A layer are linked through neurons or nodes. The output of the previous layer is used for every layer. The first is an input layer, which basically recognizes the data topic to be evaluated. Thus every layer in the ANN was fully linked with the next layers. The second layer is the secret layer, without direct contact with the external layer. The third layer is called the output layer, which results in network performance based on the data entered over the first layer [61].

ANN has the most widely used learning mode with feed-back neural propagation network (BPNN). It is a controlled learning machine

training in a reverse process. It contains of one input layer and at least one hidden layer. It's also found that any complex region of decision can be generated with two hidden layers [5]. The figure 3.6 shows a typical neural network architecture. A minimum of two input characteristics are needed in training for purposes of PD classification to avoid divergences [62].

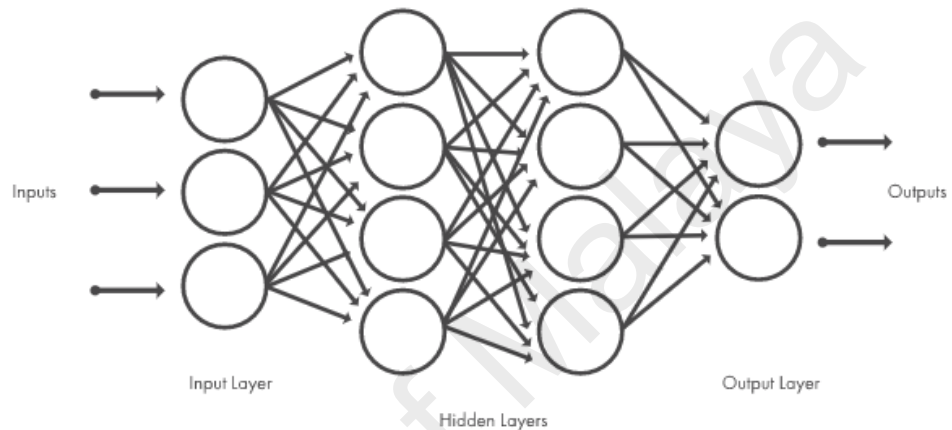


Figure 3.6 Typical neural network architecture

The "patternnet" command in the three layer feed ANN has been developed in Matlab. This ANN consists of 15 neurons in the hidden layer. This value was chosen since with lowest training time it gives the highest accuracy. The command "train" was added to the ANN. The figure 3.7 display a block diagram of the generated ANN. It was stated in the previous section that every data characteristics has been saved in "*.mat". The "*.mat file" had been loaded into the ANN to be used for the purpose of use of this input function. The performance was specified manually in binary form with a value of 1 for each class in different columns. This

work contained four different defects, so 4 different product groups were identified.

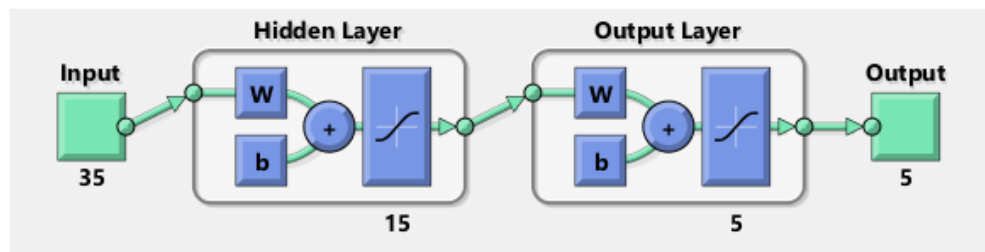


Figure 3.7 Artificial Neural Network of Feed Forward (ANN)

University of Malaysia

CHAPTER 4: DISCUSSIONS AND RESULTS

4.1 Introduction

The results of four crosslinked cable defects (XLPE) using the partial release (PD) analysis are provided in this chapter. Analysis of PD can be used by identifying the state and form of defect to evaluate the insulation quality of the cables joint. The PD measurement results were obtained. As input to the K nearest neighbor (KNN), support vector software (SVM) and artificial neural network (ANN) classifiers with discrete wavelet transformation (DWT) implemented as signal processing techniques, abstraction features were used. At the end of this chapter will shows a review of the analysis and discussion of the studies.

4.2 K Nearest Neighbor (KNN)

For a clear PD measurement and additional noise, increasing PD signal was evaluated. The signal to noise ratio (SNR) of 10, 20, 40, 60, 70, 80, 90 and 100 dB was combined with noise. Following the extraction of the input signals by discrete Wavelet Transform (DWT), K Nearest Neighbour (KNN) trained and tested the signals to identify the types of defects. Table 4.1 to Table 4.1 shows accuracy checks using KNN in various SNRs.

Table 4.1: Accuracy (%) using KNN at SNR = 10 dB

Run	Defects				Overall
	C1	C2	C3	C4	
1	100.00	100.00	96.67	100.00	99.17
2	100.00	100.00	96.67	100.00	99.17
3	96.67	100.00	100.00	100.00	99.17
4	100.00	100.00	100.00	100.00	100.00
5	96.67	100.00	100.00	100.00	99.17
6	100.00	100.00	96.67	100.00	99.17
7	100.00	100.00	100.00	100.00	100.00
8	96.67	100.00	100.00	100.00	99.17
9	100.00	100.00	100.00	100.00	100.00
10	96.67	100.00	100.00	100.00	99.17

Table 4.2: Accuracy (%) using KNN at SNR = 20 dB

Run	Defects				Overall
	C1	C2	C3	C4	
1	100.00	100.00	100.00	100.00	100.00
2	100.00	100.00	100.00	100.00	100.00
3	100.00	100.00	100.00	100.00	100.00
4	100.00	100.00	100.00	100.00	100.00
5	96.67	100.00	100.00	100.00	99.17
6	100.00	100.00	96.67	100.00	99.17
7	100.00	100.00	100.00	100.00	100.00

8	100.00	100.00	100.00	100.00	100.00
9	100.00	100.00	100.00	100.00	100.00
10	96.67	100.00	100.00	100.00	99.17

Table 4.3: Accuracy (%) using KNN at SNR = 30 dB

Run	Defects				Overall
	C1	C2	C3	C4	
1	100.00	100.00	96.67	100.00	99.17
2	93.33	100.00	96.67	100.00	97.50
3	100.00	100.00	100.00	100.00	100.00
4	100.00	100.00	96.67	100.00	99.17
5	96.67	100.00	100.00	100.00	99.17
6	100.00	100.00	100.00	100.00	100.00
7	100.00	100.00	96.67	100.00	99.17
8	100.00	100.00	96.67	100.00	99.17
9	100.00	100.00	93.33	100.00	98.33
10	100.00	100.00	96.67	100.00	99.17

Table 4.4: Accuracy (%) using KNN at SNR = 40 dB

Run	Defects				Overall
	C1	C2	C3	C4	
1	100.00	100.00	100.00	100.00	100.00
2	96.67	100.00	100.00	100.00	99.17
3	100.00	100.00	96.67	100.00	99.17

4	100.00	100.00	96.67	100.00	99.17
5	100.00	100.00	100.00	100.00	100.00
6	100.00	100.00	100.00	100.00	100.00
7	100.00	100.00	100.00	100.00	100.00
8	96.67	100.00	100.00	100.00	99.17
9	100.00	100.00	96.67	100.00	99.17
10	100.00	100.00	100.00	100.00	100.00

Table 4.5: Accuracy (%) using KNN at SNR = 50 dB

Run	Defects				Overall
	C1	C2	C3	C4	
1	100.00	100.00	96.67	100.00	99.17
2	100.00	100.00	100.00	100.00	100.00
3	100.00	100.00	96.67	100.00	99.17
4	100.00	100.00	96.67	100.00	99.17
5	100.00	100.00	96.67	100.00	99.17
6	100.00	100.00	100.00	100.00	100.00
7	100.00	100.00	100.00	100.00	100.00
8	100.00	100.00	100.00	100.00	100.00
9	100.00	100.00	100.00	100.00	100.00
10	100.00	100.00	96.67	100.00	99.17

Table 4.6: Accuracy (%) using KNN at SNR = 60 dB

Run	Defects				Overall
	C1	C2	C3	C4	
1	100.00	100.00	100.00	100.00	100.00
2	100.00	100.00	100.00	100.00	100.00
3	100.00	100.00	100.00	100.00	100.00
4	100.00	100.00	100.00	100.00	100.00
5	100.00	100.00	100.00	100.00	100.00
6	100.00	100.00	100.00	100.00	100.00
7	100.00	100.00	100.00	100.00	100.00
8	100.00	100.00	100.00	100.00	100.00
9	100.00	100.00	100.00	100.00	100.00
10	100.00	100.00	100.00	100.00	100.00

Table 4.7: Accuracy (%) using KNN at SNR = 70 dB

Run	Defects				Overall
	C1	C2	C3	C4	
1	100.00	100.00	100.00	100.00	100.00
2	100.00	100.00	100.00	100.00	100.00
3	100.00	100.00	100.00	100.00	100.00
4	100.00	100.00	100.00	100.00	100.00
5	100.00	100.00	100.00	100.00	100.00
6	100.00	100.00	100.00	100.00	100.00
7	100.00	100.00	100.00	100.00	100.00
8	100.00	100.00	100.00	100.00	100.00

9	100.00	100.00	100.00	100.00	100.00
10	100.00	100.00	100.00	100.00	100.00

Table 4.8: Accuracy (%) using KNN at SNR = 80 dB

Run	Defects				Overall
	C1	C2	C3	C4	
1	100.00	100.00	100.00	100.00	100.00
2	100.00	100.00	100.00	100.00	100.00
3	100.00	100.00	100.00	100.00	100.00
4	100.00	100.00	100.00	100.00	100.00
5	100.00	100.00	100.00	100.00	100.00
6	100.00	100.00	100.00	100.00	100.00
7	100.00	100.00	100.00	100.00	100.00
8	100.00	100.00	100.00	100.00	100.00
9	100.00	100.00	100.00	100.00	100.00
10	100.00	100.00	100.00	100.00	100.00

Table 4.9: Accuracy (%) using KNN at SNR = 90 dB

Run	Defects				Overall
	C1	C2	C3	C4	
1	100.00	100.00	100.00	100.00	100.00
2	100.00	100.00	100.00	100.00	100.00
3	100.00	100.00	100.00	100.00	100.00
4	100.00	100.00	100.00	100.00	100.00

5	100.00	100.00	100.00	100.00	100.00
6	100.00	100.00	100.00	100.00	100.00
7	100.00	100.00	100.00	100.00	100.00
8	100.00	100.00	100.00	100.00	100.00
9	100.00	100.00	100.00	100.00	100.00
10	100.00	100.00	100.00	100.00	100.00

Table 4.10: Accuracy (%) using KNN at SNR = 100 dB

Run	Defects				Overall
	C1	C2	C3	C4	
1	100.00	100.00	100.00	100.00	100.00
2	100.00	100.00	100.00	100.00	100.00
3	100.00	100.00	100.00	100.00	100.00
4	100.00	100.00	100.00	100.00	100.00
5	100.00	100.00	100.00	100.00	100.00
6	100.00	100.00	100.00	100.00	100.00
7	100.00	100.00	100.00	100.00	100.00
8	100.00	100.00	100.00	100.00	100.00
9	100.00	100.00	100.00	100.00	100.00
10	100.00	100.00	100.00	100.00	100.00

4.3 Support Vector Machine (SVM)

For a simple PD measurement and additional noise, every PD signal was analyzed. The noise-to-noise ratio (SNR) was 10, 20, 40, 60, 70, 80, 90 and 100 dB in accordance with the signals. After discrete transform wavelet signals were eliminated (DWT), they were trained and tested to identify types of deficiency by Support Vector Machine (SVM). Table 4.11 to Table 4.20 shows the results of accuracy utilizing SVM in different SNRs.

Table 4.11: Accuracy (%) using SVM at SNR = 10 dB

Run	Defects				Overall
	C1	C2	C3	C4	
1	100.00	100.00	0.00	0.00	50.00
2	100.00	100.00	0.00	0.00	50.00
3	100.00	96.67	0.00	0.00	49.17
4	100.00	100.00	0.00	0.00	50.00
5	100.00	100.00	3.33	0.00	50.83
6	100.00	96.67	0.00	0.00	49.17
7	100.00	96.67	0.00	0.00	49.17
8	100.00	96.67	0.00	0.00	49.17
9	100.00	100.00	6.67	0.00	51.67
10	100.00	96.67	0.00	0.00	49.17

Table 4.12: Accuracy (%) using SVM at SNR = 20 dB

Run	Defects				Overall
	C1	C2	C3	C4	
1	100.00	100.00	0.00	0.00	50.00
2	100.00	100.00	0.00	0.00	50.00
3	100.00	96.67	0.00	0.00	49.17
4	100.00	96.67	6.67	0.00	50.83
5	100.00	90.00	3.33	0.00	48.33
6	100.00	96.67	0.00	0.00	49.17
7	100.00	93.33	0.00	0.00	48.33
8	100.00	100.00	0.00	0.00	50.00
9	100.00	100.00	0.00	0.00	50.00
10	100.00	96.67	3.33	0.00	50.00

Table 4.13: Accuracy (%) using SVM at SNR = 30 dB

Run	Defects				Overall
	C1	C2	C3	C4	
1	100.00	100.00	0.00	0.00	50.00
2	100.00	96.67	0.00	0.00	49.17
3	100.00	100.00	3.33	0.00	50.83
4	100.00	96.67	0.00	0.00	49.17
5	100.00	100.00	3.33	0.00	50.83
6	100.00	93.33	0.00	0.00	48.33
7	100.00	100.00	0.00	0.00	50.00

8	100.00	100.00	0.00	0.00	50.00
9	100.00	96.67	0.00	0.00	49.17
10	100.00	100.00	6.67	0.00	51.67

Table 4.14: Accuracy (%) using SVM at SNR = 40 dB

Run	Defects				Overall
	C1	C2	C3	C4	
1	100.00	100.00	0.00	0.00	50.00
2	100.00	93.33	0.00	0.00	48.33
3	100.00	100.00	0.00	0.00	50.00
4	100.00	100.00	0.00	0.00	50.00
5	100.00	100.00	0.00	0.00	50.00
6	100.00	100.00	0.00	0.00	50.00
7	100.00	96.67	0.00	0.00	49.17
8	100.00	100.00	0.00	0.00	50.00
9	100.00	96.67	0.00	0.00	49.17
10	100.00	100.00	0.00	0.00	50.00

Table 4.15: Accuracy (%) using SVM at SNR = 50 dB

Run	Defects				Overall
	C1	C2	C3	C4	
1	100.00	100.00	0.00	0.00	50.00
2	100.00	100.00	0.00	0.00	50.00
3	100.00	100.00	0.00	0.00	50.00

4	100.00	100.00	0.00	0.00	50.00
5	100.00	100.00	0.00	0.00	50.00
6	100.00	100.00	0.00	0.00	50.00
7	100.00	100.00	0.00	0.00	50.00
8	100.00	100.00	3.33	0.00	50.83
9	100.00	100.00	0.00	0.00	50.00
10	100.00	100.00	3.33	0.00	50.83

Table 4.16: Accuracy (%) using SVM at SNR = 60 dB

Run	Defects				Overall
	C1	C2	C3	C4	
1	100.00	100.00	0.00	0.00	50.00
2	100.00	100.00	0.00	0.00	50.00
3	100.00	100.00	0.00	0.00	50.00
4	100.00	100.00	3.33	0.00	50.83
5	100.00	100.00	0.00	0.00	50.00
6	100.00	100.00	0.00	0.00	50.00
7	100.00	100.00	0.00	0.00	50.00
8	100.00	100.00	0.00	0.00	50.00
9	100.00	100.00	0.00	0.00	50.00
10	100.00	100.00	3.33	0.00	50.83

Table 4.17: Accuracy (%) using SVM at SNR = 70 dB

Run	Defects				Overall
	C1	C2	C3	C4	
1	100.00	100.00	0.00	0.00	50.00
2	100.00	100.00	0.00	0.00	50.00
3	100.00	100.00	3.33	0.00	50.83
4	100.00	100.00	0.00	0.00	50.00
5	100.00	100.00	0.00	0.00	50.00
6	100.00	100.00	0.00	0.00	50.00
7	100.00	100.00	0.00	0.00	50.00
8	100.00	100.00	0.00	0.00	50.00
9	100.00	100.00	3.33	0.00	50.83
10	100.00	100.00	0.00	0.00	50.00

Table 4.18: Accuracy (%) using SVM at SNR = 80 dB

Run	Defects				Overall
	C1	C2	C3	C4	
1	100.00	100.00	6.67	0.00	51.67
2	100.00	100.00	6.67	0.00	51.67
3	100.00	100.00	3.33	0.00	50.83
4	100.00	100.00	3.33	0.00	50.83
5	0.00	100.00	3.33	0.00	50.83
6	100.00	100.00	0.00	0.00	50.00
7	100.00	100.00	3.33	0.00	50.83
8	100.00	100.00	3.33	0.00	50.83

9	100.00	100.00	6.67	0.00	51.67
10	100.00	100.00	6.67	0.00	51.67

Table 4.19: Accuracy (%) using SVM at SNR = 90 dB

Run	Defects				Overall
	C1	C2	C3	C4	
1	100.00	100.00	3.33	0.00	50.83
2	100.00	100.00	0.00	0.00	50.00
3	100.00	100.00	3.33	0.00	50.83
4	100.00	100.00	3.33	0.00	50.83
5	0.00	100.00	100.00	0.00	50.00
6	100.00	100.00	6.67	0.00	51.67
7	100.00	100.00	6.67	0.00	51.67
8	100.00	100.00	6.67	0.00	51.67
9	100.00	100.00	0.00	0.00	50.00
10	100.00	100.00	0.00	0.00	50.00

Table 4.20: Accuracy (%) using SVM at SNR = 100 dB

Run	Defects				Overall
	C1	C2	C3	C4	
1	100.00	100.00	3.33	0.00	50.83
2	100.00	100.00	3.33	0.00	50.83
3	100.00	100.00	3.33	0.00	50.83

4	100.00	100.00	3.33	0.00	50.83
5	100.00	100.00	0.00	0.00	50.00
6	100.00	100.00	3.33	0.00	50.83
7	100.00	100.00	0.00	0.00	50.00
8	100.00	100.00	6.67	0.00	51.67
9	100.00	100.00	0.00	0.00	50.00
10	100.00	100.00	6.67	0.00	51.67

4.4 Artificial Neural Network (ANN)

For a clear PD measurement and additional noise, increasing PD signal was analyzed. The signal to noise ratio (SNR) of 10, 20, 40, 60, 70, 80, 90 and 100 dB is coupled with the noise. The signals were trained and tested through artificial neural network (ANN), when they had been extracted via discrete wavelet transformation (DWT). The fault types were identified. Table 4.21 to Table 4.30 shows the accuracy outcomes using ANN under various SNRs.

Table 4.21: Accuracy (%) using ANN at SNR = 10 dB

Run	Defects				Overall
	C1	C2	C3	C4	
1	0.00	100.00	100.00	0.00	50.00
2	0.00	93.33	100.00	0.00	48.33
3	0.00	96.67	100.00	0.00	49.17
4	100.00	100.00	96.67	100.00	99.17
5	100.00	100.00	100.00	100.00	100.00

6	0.00	100.00	100.00	0.00	50.00
7	0.00	96.67	100.00	0.00	49.17
8	0.00	93.33	100.00	0.00	48.33
9	0.00	93.33	100.00	0.00	48.33
10	0.00	100.00	100.00	0.00	50.00

Table 4.22: Accuracy (%) using ANN at SNR = 20 dB

Run	Defects				Overall
	C1	C2	C3	C4	
1	0.00	100.00	100.00	0.00	50.00
2	0.00	100.00	0.00	0.00	25.00
3	0.00	93.33	100.00	0.00	48.33
4	0.00	96.67	100.00	0.00	49.17
5	0.00	96.67	100.00	0.00	49.17
6	100.00	100.00	100.00	100.00	100.00
7	0.00	96.67	100.00	0.00	49.17
8	0.00	100.00	100.00	0.00	50.00
9	0.00	100.00	100.00	0.00	50.00
10	0.00	96.67	100.00	0.00	49.17

Table 4.23: Accuracy (%) using ANN at SNR = 30 dB

Run	Defects				Overall
	C1	C2	C3	C4	
1	100.00	100.00	96.67	100.00	99.17

2	0.00	100.00	100.00	0.00	50.00
3	0.00	96.67	100.00	0.00	49.17
4	0.00	100.00	73.33	0.00	43.33
5	0.00	93.33	100.00	0.00	43.33
6	100.00	100.00	96.67	100.00	99.17
7	0.00	100.00	100.00	0.00	50.00
8	0.00	96.67	100.00	0.00	49.17
9	0.00	100.00	0.00	0.00	25.00
10	0.00	100.00	100.00	0.00	50.00

Table 4.24: Accuracy (%) using ANN at SNR = 40 dB

Run	Defects				Overall
	C1	C2	C3	C4	
1	0.00	100.00	100.00	0.00	50.00
2	100.00	100.00	100.00	100.00	100.00
3	0.00	100.00	100.00	0.00	50.00
4	100.00	100.00	96.67	100.00	99.17
5	0.00	100.00	96.67	0.00	49.17
6	100.00	100.00	96.67	100.00	99.17
7	0.00	100.00	0.00	0.00	25.00
8	0.00	100.00	100.00	0.00	50.00
9	0.00	100.00	100.00	0.00	50.00
10	0.00	93.33	100.00	0.00	48.33

Table 4.25: Accuracy (%) using ANN at SNR = 50 dB

Run	Defects				Overall
	C1	C2	C3	C4	
1	100.00	100.00	100.00	100.00	100.00
2	0.00	100.00	100.00	0.00	50.00
3	100.00	96.67	100.00	100.00	99.17
4	0.00	100.00	100.00	0.00	50.00
5	0.00	100.00	100.00	0.00	50.00
6	100.00	100.00	100.00	100.00	100.00
7	100.00	100.00	100.00	100.00	100.00
8	100.00	100.00	100.00	100.00	100.00
9	56.67	100.00	86.67	100.00	85.83
10	100.00	100.00	100.00	100.00	100.00

Table 4.26: Accuracy (%) using ANN at SNR = 60 dB

Run	Defects				Overall
	C1	C2	C3	C4	
1	100.00	100.00	100.00	100.00	100.00
2	0.00	100.00	100.00	0.00	50.00
3	96.67	100.00	100.00	100.00	99.17
4	100.00	100.00	100.00	100.00	100.00
5	96.67	100.00	100.00	100.00	99.17
6	0.00	100.00	100.00	0.00	50.00
7	0.00	100.00	100.00	0.00	50.00
8	0.00	100.00	100.00	0.00	50.00

9	0.00	100.00	100.00	0.00	50.00
10	100.00	100.00	100.00	100.00	100.00

Table 4.27: Accuracy (%) using ANN at SNR = 70 dB

Run	Defects				Overall
	C1	C2	C3	C4	
1	0.00	100.00	100.00	0.00	50.00
2	100.00	100.00	100.00	100.00	100.00
3	100.00	100.00	100.00	100.00	100.00
4	0.00	100.00	100.00	0.00	50.00
5	0.00	100.00	100.00	0.00	50.00
6	0.00	100.00	100.00	0.00	50.00
7	0.00	100.00	100.00	0.00	50.00
8	0.00	100.00	100.00	0.00	50.00
9	0.00	100.00	100.00	0.00	50.00
10	0.00	100.00	100.00	0.00	50.00

Table 4.28: Accuracy (%) using ANN at SNR = 80 dB

Run	Defects				Overall
	C1	C2	C3	C4	
1	0.00	96.67	100.00	96.67	49.17
2	93.33	100.00	100.00	100.00	98.33
3	100.00	100.00	100.00	100.00	100.00
4	0.00	100.00	100.00	0.00	50.00

5	0.00	100.00	100.00	0.00	50.00
6	0.00	100.00	100.00	0.00	50.00
7	0.00	100.00	100.00	0.00	50.00
8	96.67	100.00	100.00	100.00	99.17
9	100.00	100.00	100.00	100.00	100.00
10	0.00	100.00	100.00	0.00	50.00

Table 4.29: Accuracy (%) using ANN at SNR = 90 dB

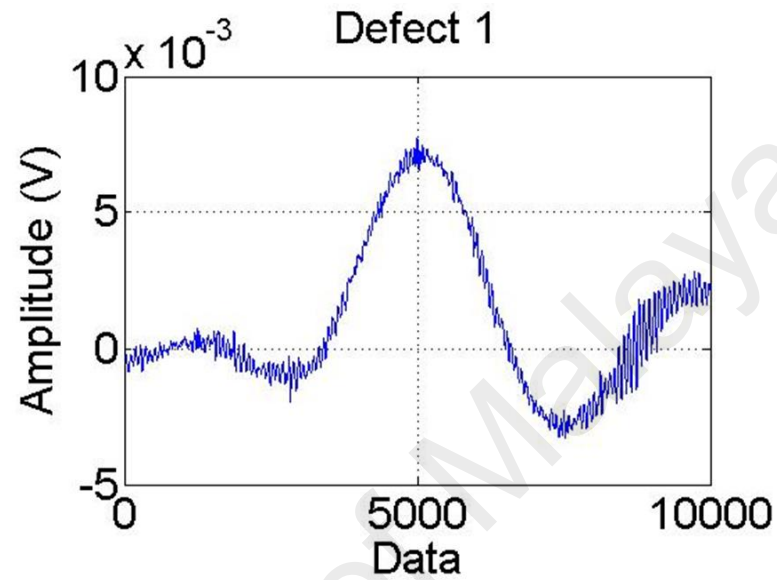
Run	Defects				Overall
	C1	C2	C3	C4	
1	0.00	100.00	100.00	0.00	50.00
2	0.00	100.00	100.00	0.00	50.00
3	0.00	100.00	100.00	0.00	50.00
4	0.00	100.00	100.00	0.00	50.00
5	0.00	100.00	100.00	0.00	50.00
6	0.00	96.67	100.00	0.00	49.17
7	100.00	100.00	100.00	100.00	100.00
8	0.00	100.00	100.00	0.00	50.00
9	0.00	100.00	100.00	0.00	50.00
10	100.00	100.00	100.00	100.00	100.00

Table 4.30: Accuracy (%) using ANN at SNR = 100 dB

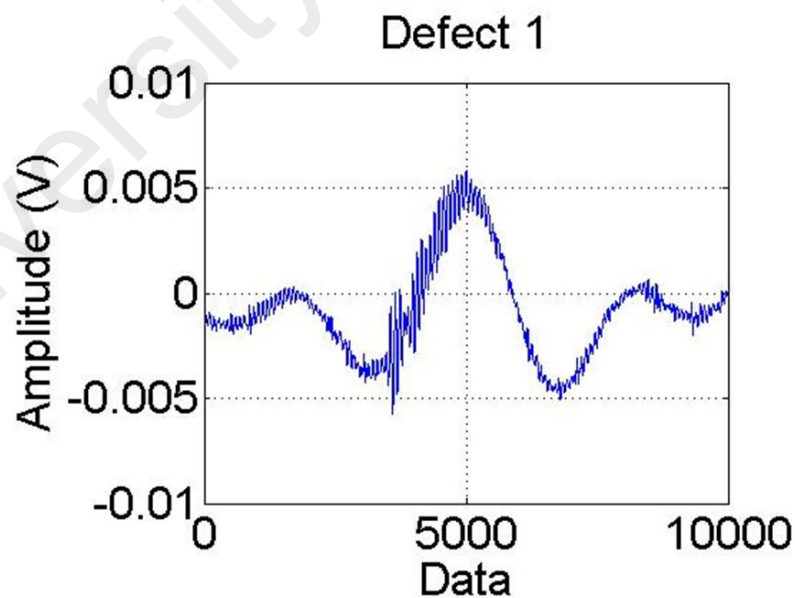
Run	Defects				Overall
	C1	C2	C3	C4	
1	0.00	100.00	100.00	0.00	50.00
2	0.00	100.00	100.00	0.00	50.00
3	80.00	100.00	100.00	100.00	95.00
4	0.00	100.00	100.00	0.00	50.00
5	0.00	100.00	100.00	0.00	50.00
6	90.00	100.00	100.00	100.00	97.50
7	100.00	100.00	100.00	100.00	100.00
8	0.00	100.00	100.00	0.00	50.00
9	0.00	100.00	100.00	0.00	50.00
10	100.00	100.00	100.00	100.00	100.00

4.5 PD Signals After DWT

Figure 4.1 to Figure 4.4 shows a clear Input signal and a distorted PD signal accompanying DWT for C1 defect (insulation incision defect), C2 defect (axial path shift defect), C3 (semiconductor layer tip defect) and C4 (metal particle on XLPE defect).

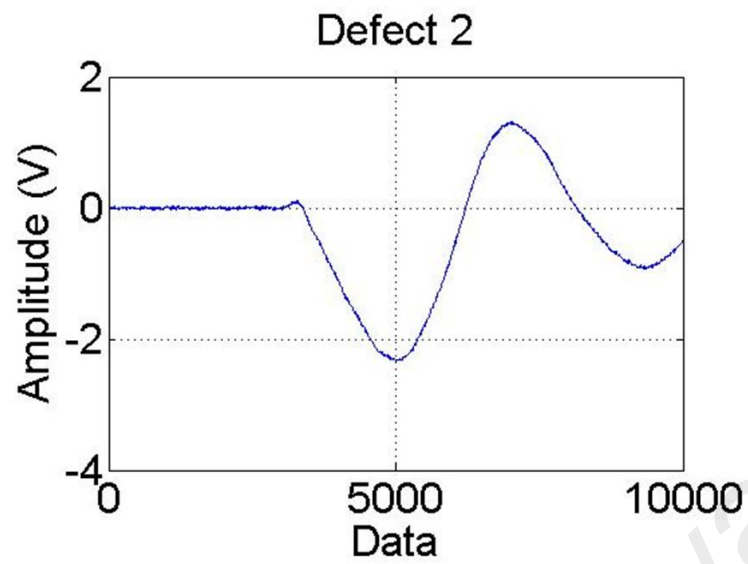


(a)

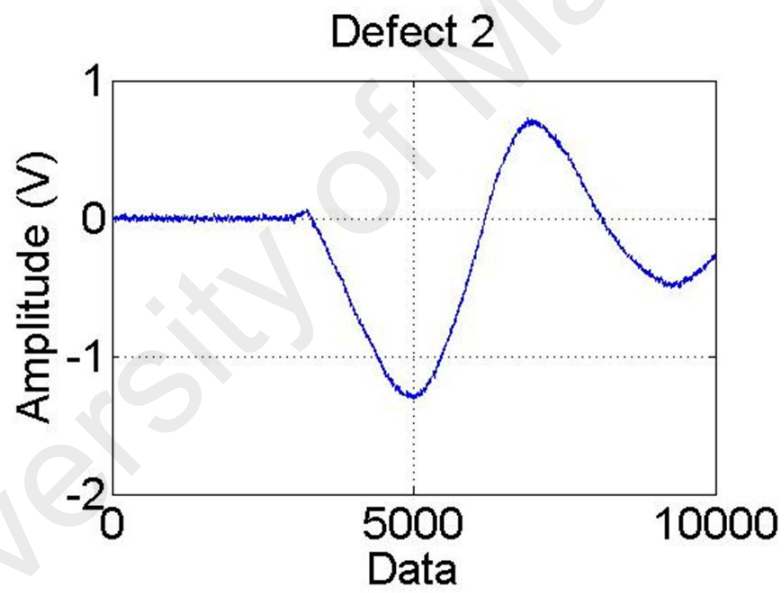


(b)

Figure 4.1 (a) Clean PD signal and (b) noisy PD signal after DWT for defect C1 (insulation incision defect)

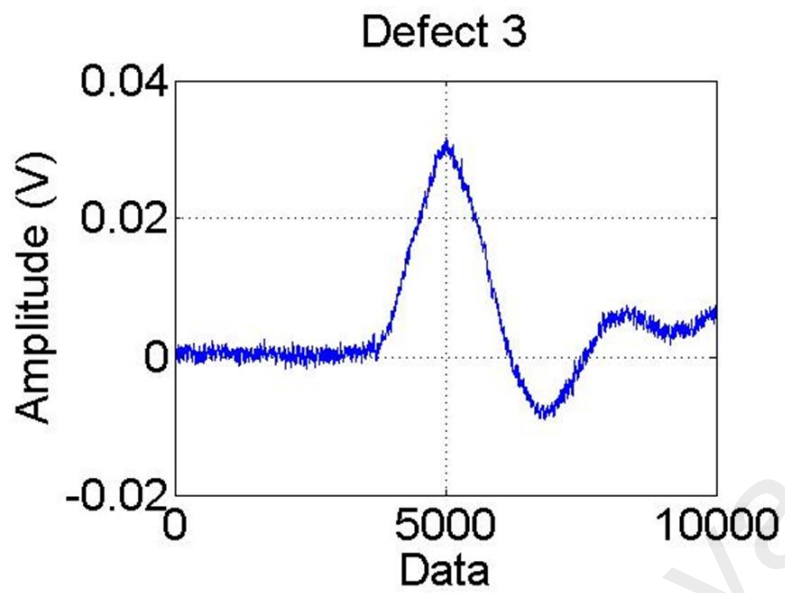


(a)

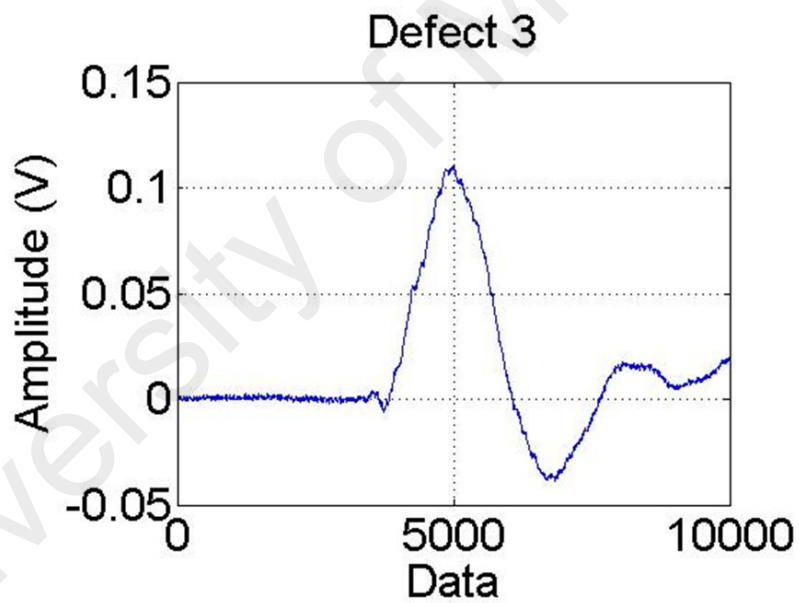


(b)

Figure 4.2: (a) Clean PD signal and (b) noisy PD signal after DWT for defect C2 (axial path shift defect)

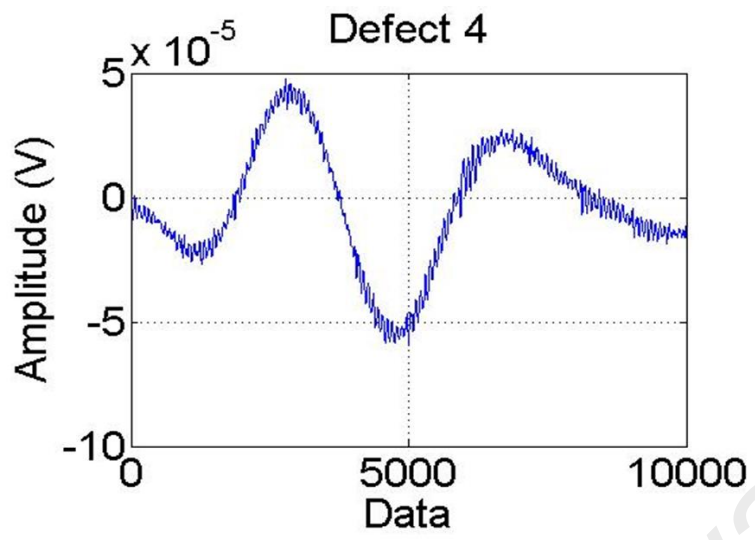


(a)

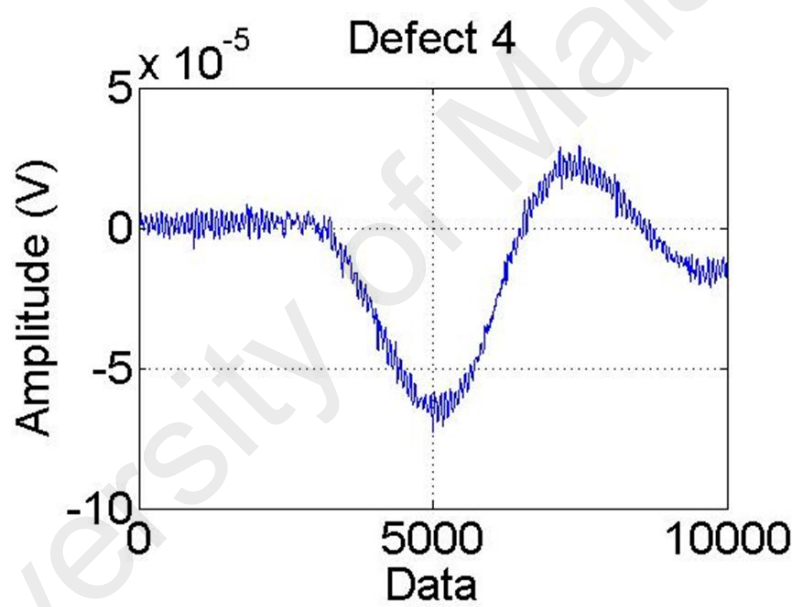


(b)

Figure 4.3: (a) Clean PD signal and (b) noisy PD signal after DWT for defect C3 (semiconductor layer tip defect)



(a)



(b)

Figure 4.4: (a) Clean PD signal and (b) noisy PD signal after DWT for defect C4 (Metal particle on XLPE defect)

4.6 Classification Results

A contrast with DWT as the signal processing system under a particular signal to noise ratio (SNR) is shown in Table 4.31. The approaches used in the previous work are ANN and SVM [62] while using KNN is the method proposed in this work. Every procedure was repeated for 10 times using training and testing data taken randomly and the accuracy rate has been obtained. Through this table, it has been shown that KNN provides the highest performance of defect classification on XLPE cables, where 100 percent for SNR from 60 dB to 100 dB and 99.42 percent for SNR at 10 dB, 99.75 percent for 20 dB, 99.08 percent for 30 dB and 99.58 percent for 50 dB. The exactness of the defect type evaluation for the three methods is greater in the higher SNR. It can also be seen that KNN achieves greater accuracy in signals at various levels of noise relative to SVM and ANN, which in turn declines specifically at higher levels of noise.

Table 4.31: Comparison of accuracy (%) between different classifiers

Classifier	Accuracy (%)									
	Signal to Noise Ratio (SNR) (dB)									
	10	20	30	40	50	60	70	80	90	100
KNN	99.42	99.75	99.08	99.58	99.58	100.00	100.00	100.00	100.00	100.00
SVM	49.83	49.58	49.92	49.67	50.17	50.17	50.17	51.08	50.75	50.75
ANN	59.25	52.00	56.33	62.08	83.50	74.83	60.00	69.67	59.92	69.25

CHAPTER 5: RECOMMENDATIONS AND CONCLUSIONS

5.1 Conclusions

A successful classification of defect types in cable joints of KNN with cross link polyethylene (XLPE) has been achieved. The obtained PD inputs were collected with discrete signal transform (DWT) methods. This designs were effectively used for the purpose of defining defect types in XLPE cable connectors for k nearest neighbor (KNN), the support vectors (SVM) and artificial neural networks (ANN).

To assess the correct approach with the greatest accuracy, the same outcomes from the different approaches were contrasted with each other. The results show that the extracted input characteristic from the discrete wavelet transform (DWT) signals, classified using the K Nearest Neighbor classifier (KNN), was able to classify the defect types with the greatest precision. A contrast of the SVM and ANN reveals also that the data obtained from this work are higher as the results are more accurate.

The extraction of PD signals from the DWT technology and the KNN training can therefore be considered as an appropriate tool for classifying fault forms in XLPE cable connections that can assist in cable joint maintenance and detection.

5.2 Recommendations on future work

Following are the initial work that can be carried throughout this research:

- I. Develop a PD classifier that is capable of modeling data sequence so that each sample can be presumed to be based on the previous ones used with convolutional layers to expand the effective pixel neighborhood
- II. Test with other signal processing methods
- III. Classify using other classifiers

University of Malaya

REFERENCES

- [1] Y. Tian, P. L. Lewin, and A. E. Davies, "Comparison of on-line partial discharge detection methods for HV cable joints," *IEEE Transactions on Dielectrics and Electrical Insulation*, vol. 9, no. 4, pp. 604-615, 2002, doi: 10.1109/TDEI.2002.1024439.
- [2] M. Chen, J. Chen, and C. Cheng, "Partial discharge detection by RF coil in 161 kV power transformer," *IEEE Transactions on Dielectrics and Electrical Insulation*, vol. 21, no. 3, pp. 1405-1414, 2014, doi: 0.1109/TDEI.2014.6832289.
- [3] Y.-S. Cho, M.-J. Shim, and S.-W. Kim, "Electrical tree initiation mechanism of artificial defects filled XLPE," *Materials Chemistry and Physics*, vol. 56, no. 1, pp. 87-90, 1998/09/30/ 1998, doi: 10.1016/S0254-0584(98)00160-6.
- [4] J. A. Hunter, P. L. Lewin, L. Hao, C. Walton, and M. Michel, "Autonomous classification of PD sources within three-phase 11 kV PILC cables," *IEEE Transactions on Dielectrics and Electrical Insulation*, vol. 20, no. 6, pp. 2117-2124, 2013, doi: 10.1109/TDEI.2013.6678860.
- [5] L. Satish and W. S. Zaengl, "Artificial neural networks for recognition of 3-d partial discharge patterns," *IEEE Transactions on Dielectrics and Electrical Insulation*, vol. 1, no. 2, pp. 265-275, 1994, doi: 10.1109/94.300259.
- [6] L. Angrisani, P. Daponte, G. Lupò, C. Petrarca, and M. Vitelli, "Analysis of ultrawide-band detected partial discharges by means of a multiresolution digital signal-processing method," *Measurement*, vol. 27, no. 3, pp. 207-221, 2000/04/01/ 2000, doi: 10.1016/S0263-2241(99)00067-6.
- [7] L. Satish and B. I. Gururaj, "Partial discharge pattern classification using multilayer neural networks," *IEE Proceedings A - Science, Measurement and Technology*, vol. 140, no. 4, pp. 323-330, 1993, doi: 10.1049/ip-a-3.1993.0049.
- [8] B. Karthikeyan, S. Gopal, and S. Venkatesh, "ART 2—an unsupervised neural network for PD pattern recognition and classification," *Expert Systems with Applications*, vol. 31, no. 2, pp. 345-350, 2006/08/01/ 2006, doi: 10.1016/j.eswa.2005.09.029.
- [9] H. d. O. Mota, L. C. D. d. Rocha, T. C. d. M. Salles, and F. H. Vasconcelos, "Partial discharge signal denoising with spatially adaptive wavelet thresholding and support vector machines," *Electric Power Systems Research*, vol. 81, no. 2, pp. 644-659, 2011/02/01/ 2011, doi: 10.1016/j.epsr.2010.10.030.
- [10] H. Ilias, Y. Teo Soon, A. H. A. Bakar, H. Mokhlis, G. Chen, and P. L. Lewin, "Partial discharge patterns in high voltage insulation," in *2012 IEEE International Conference on Power and Energy (PECon)*, 2-5 Dec. 2012 2012, pp. 750-755, doi: 10.1109/PECon.2012.6450316.

- [11] F. H. Kreuger, *Industrial high voltage*. Delft, the Netherlands: Delft University Press (in English), 1991.
- [12] X. Chen, Y. Xu, and X. Cao, "Nonlinear time series analysis of partial discharges in electrical trees of XLPE cable insulation samples," *IEEE Transactions on Dielectrics and Electrical Insulation*, vol. 21, no. 4, pp. 1455-1461, 2014, doi: 10.1109/TDEI.2014.004307.
- [13] M. Ghaffarian, "Partial Discharge Signatures of Defects in Insulation Systems Consisting of Oil and Oil-impregnated Paper," 2012.
- [14] C. Q. Su and C. R. Li, "Using very-low-frequency and oscillating-wave tests to improve the reliability of distribution cables," *IEEE Electrical Insulation Magazine*, vol. 29, no. 1, pp. 38-45, 2013, doi: 10.1109/MEI.2013.6410538.
- [15] F. Wester, E. Gulski, J. Smit, and E. Groot, *PD knowledge rules support for CBM of distribution power cables*. 2002, pp. 66-69.
- [16] D. Evagorou *et al.*, "Feature extraction of partial discharge signals using the wavelet packet transform and classification with a probabilistic neural network," *IET Science, Measurement & Technology*, vol. 4, no. 3, pp. 177-192, 2010, doi: 10.1049/iet-smt.2009.0023.
- [17] B. Hui, C. Liu, Y. Tian, M. Fu, Y. Xu, and Y. Zhang, "The relationship between partial discharge behavior and the degradation of 10 kV XLPE cable joints," in *2016 International Conference on Condition Monitoring and Diagnosis (CMD)*, 25-28 Sept. 2016 2016, pp. 843-846, doi: 10.1109/CMD.2016.7758006.
- [18] G. C. Montanari, A. Cavallini, and F. Puletti, "A new approach to partial discharge testing of HV cable systems," *IEEE Electrical Insulation Magazine*, vol. 22, no. 1, pp. 14-23, 2006, doi: 10.1109/MEI.2006.1618967.
- [19] H. Zhang, T. R. Blackburn, B. t. Phung, and D. Sen, "A novel wavelet transform technique for on-line partial discharge measurements. 1. WT de-noising algorithm," *IEEE Transactions on Dielectrics and Electrical Insulation*, vol. 14, no. 1, pp. 3-14, 2007, doi: 10.1109/TDEI.2007.302864.
- [20] F. a. J. G. Jay, "IEEE Standard Dictionary of Electrical and Electronics Terms," *IEEE Transactions on Power Apparatus and Systems*, vol. PAS-99, no. 6, pp. 37a-37a, 1980, doi: 10.1109/TPAS.1980.319816.
- [21] F. H. Kreuger, E. Gulski, and A. Krivda, "Classification of partial discharges," *IEEE Transactions on Electrical Insulation*, vol. 28, no. 6, pp. 917-931, 1993, doi: 10.1109/14.249365.
- [22] P. Casals-Torrens, A. González-Parada, and R. Bosch-Tous, "Online PD detection on high voltage underground power cables by acoustic emission," *Procedia Engineering*, vol. 35, pp. 22-30, 2012/01/01/ 2012, doi: 10.1016/j.proeng.2012.04.161.
- [23] P. Kundu, N. K. Kishore, and A. K. Sinha, "Identification of two simultaneous partial discharge sources in an oil-pressboard insulation system using acoustic

emission techniques," *Applied Acoustics*, vol. 73, no. 4, pp. 395-401, 2012/04/01/ 2012, doi: 10.1016/j.apacoust.2011.11.004.

- [24] N. A. Al-geelani, M. A. M. Piah, Z. Adzis, and M. A. Algeelani, "Hybrid regrouping PSO based wavelet neural networks for characterization of acoustic signals due to surface discharges on H.V. glass insulators," *Applied Soft Computing*, vol. 13, no. 12, pp. 4622-4632, 2013/12/01/ 2013, doi: 10.1016/j.asoc.2013.07.011.
- [25] C. Boya, M. Ruiz-Llata, J. Posada, and J. A. Garcia-Souto, "Identification of multiple partial discharge sources using acoustic emission technique and blind source separation," *IEEE Transactions on Dielectrics and Electrical Insulation*, vol. 22, no. 3, pp. 1663-1673, 2015, doi: 10.1109/TDEI.2015.7116363.
- [26] H. Suzuki and T. Endoh, "Pattern recognition of partial discharge in XLPE cables using a neural network," in *[1991] Proceedings of the 3rd International Conference on Properties and Applications of Dielectric Materials*, 8-12 July 1991 1991, pp. 43-46 vol.1, doi: 10.1109/ICPADM.1991.172350.
- [27] T. Boczar, S. Borucki, A. Cichon, and D. Zmarzly, "Application Possibilities of Artificial Neural Networks for Recognizing Partial Discharges Measured by the Acoustic Emission Method," *IEEE Transactions on Dielectrics and Electrical Insulation*, vol. 16, no. 1, pp. 214-223, 2009, doi: 10.1109/TDEI.2009.4784570.
- [28] S. Venkatesh and S. Gopal, "Robust Heteroscedastic Probabilistic Neural Network for multiple source partial discharge pattern recognition – Significance of outliers on classification capability," *Expert Systems with Applications*, vol. 38, no. 9, pp. 11501-11514, 2011/09/01/ 2011, doi: 10.1016/j.eswa.2011.03.026.
- [29] F.-C. Gu, H.-C. Chang, F.-H. Chen, and C.-C. Kuo, "Partial discharge pattern recognition of power cable joints using extension method with fractal feature enhancement," *Expert Systems with Applications*, vol. 39, no. 3, pp. 2804-2812, 2012/02/15/ 2012, doi: 10.1016/j.eswa.2011.08.140.
- [30] I. Y. Shurrab, A. H. El-Hag, K. Assaleh, R. A. Ghunem, and S. Jayaram, "RF-based monitoring and classification of partial discharge on wet silicone rubber surface," *IEEE Transactions on Dielectrics and Electrical Insulation*, vol. 20, no. 6, pp. 2188-2194, 2013, doi: 10.1109/TDEI.2013.6678869.
- [31] A. Abubakar Mas'ud, B. G. Stewart, and S. G. McMeekin, "Application of an ensemble neural network for classifying partial discharge patterns," *Electric Power Systems Research*, vol. 110, pp. 154-162, 2014/05/01/ 2014, doi: 10.1016/j.epsr.2014.01.010.
- [32] H. H. Sinaga, B. T. Phung, and T. R. Blackburn, "Neuro fuzzy recognition of ultra-high frequency partial discharges in transformers," in *2010 Conference Proceedings IPEC*, 27-29 Oct. 2010 2010, pp. 346-351, doi: 10.1109/IPECON.2010.5697156.
- [33] L. Li, J. Tang, and Y. Liu, "Partial discharge recognition in gas insulated switchgear based on multi-information fusion," *IEEE Transactions on Dielectrics*

and *Electrical Insulation*, vol. 22, no. 2, pp. 1080-1087, 2015, doi: 10.1109/TDEI.2015.7076809.

- [34] T. R. Sukma *et al.*, "Classification of Partial Discharge Sources using Waveform Parameters and Phase-Resolved Partial Discharge Pattern as Input for the Artificial Neural Network," in *2018 Condition Monitoring and Diagnosis (CMD)*, 23-26 Sept. 2018 2018, pp. 1-6, doi: 10.1109/CMD.2018.8535675.
- [35] L. Hao, P. L. Lewin, and S. J. Dodd, "Comparison of support vector machine based partial discharge identification parameters," in *Conference Record of the 2006 IEEE International Symposium on Electrical Insulation*, 11-14 June 2006 2006, pp. 110-113, doi: 10.1109/ELINSL.2006.1665269.
- [36] R. M. Sharkawy, R. S. Mangoubi, T. k. Abdel-Galil, M. M. A. Salama, and R. Bartnikas, "SVM classification of contaminating particles in liquid dielectrics using higher order statistics of electrical and acoustic PD measurements," *IEEE Transactions on Dielectrics and Electrical Insulation*, vol. 14, no. 3, pp. 669-678, 2007, doi: 10.1109/TDEI.2007.369530.
- [37] S. Wenrong, L. Junhao, Y. Peng, and L. Yanming, "Digital detection, grouping and classification of partial discharge signals at DC voltage," *IEEE Transactions on Dielectrics and Electrical Insulation*, vol. 15, no. 6, pp. 1663-1674, 2008, doi: 10.1109/TDEI.2008.4712671.
- [38] L. Hao and P. L. Lewin, "Partial discharge source discrimination using a support vector machine," *IEEE Transactions on Dielectrics and Electrical Insulation*, vol. 17, no. 1, pp. 189-197, 2010, doi: 10.1109/TDEI.2010.5412017.
- [39] X. Zhang, S. Xiao, N. Shu, J. Tang, and W. Li, "GIS partial discharge pattern recognition based on the chaos theory," *IEEE Transactions on Dielectrics and Electrical Insulation*, vol. 21, no. 2, pp. 783-790, 2014, doi: 10.1109/TDEI.2013.004020.
- [40] Y. Khan, A. A. Khan, F. N. Budiman, A. Beroual, N. H. Malik, and A. A. Al-Arainy, "Partial discharge pattern analysis using support vector machine to estimate size and position of metallic particle adhering to spacer in GIS," *Electric Power Systems Research*, vol. 116, pp. 391-398, 2014/11/01/ 2014, doi: 10.1016/j.epsr.2014.07.001.
- [41] Y. Ling, D. Bai, M. Wang, X. Gong, and C. Gu, "SVM-based Partial Discharge Pattern Classification for GIS," *Journal of Physics: Conference Series*, vol. 960, p. 012051, 01/01 2018, doi: 10.1088/1742-6596/960/1/012051.
- [42] L. Gaoyang, R. Mingzhe, W. Xiaohua, L. Xi, and L. Yunjia, "Partial discharge patterns recognition with deep Convolutional Neural Networks," in *2016 International Conference on Condition Monitoring and Diagnosis (CMD)*, 25-28 Sept. 2016 2016, pp. 324-327, doi: 10.1109/CMD.2016.7757816.
- [43] Y. Lu, R. Wei, J. Chen, and J. Yuan, "Convolutional Neural Network Based Transient Earth Voltage Detection," in *2016 15th International Symposium on Parallel and Distributed Computing (ISPDC)*, 8-10 July 2016 2016, pp. 386-389, doi: 10.1109/ISPDC.2016.65.

- [44] G. Huang, W. Cao, X. Xie, Z. Li, Z. Li, and G. Sheng, "Classification of Partial Discharge Images within DC XLPE Cables Based on Convolutional Deep Belief Network," in *2018 Condition Monitoring and Diagnosis (CMD)*, 23-26 Sept. 2018 2018, pp. 1-4, doi: 10.1109/CMD.2018.8535602.
- [45] Z. Yufeng, X. Yongpeng, C. Jingde, F. Rusen, S. Gehao, and J. Xiuchen, "Partial discharge pattern recognition of DC XLPE cables based on convolutional neural network," in *2018 Condition Monitoring and Diagnosis (CMD)*, 23-26 Sept. 2018 2018, pp. 1-6, doi: 10.1109/CMD.2018.8535793.
- [46] X. Peng *et al.*, "A Convolutional Neural Network-Based Deep Learning Methodology for Recognition of Partial Discharge Patterns from High-Voltage Cables," *IEEE Transactions on Power Delivery*, vol. 34, no. 4, pp. 1460-1469, 2019, doi: 10.1109/TPWRD.2019.2906086.
- [47] L. Cai, N. F. Thornhill, S. Kuenzel, and B. C. Pal, "Real-Time Detection of Power System Disturbances Based on k -Nearest Neighbor Analysis," *IEEE Access*, vol. 5, pp. 5631-5639, 2017, doi: 10.1109/ACCESS.2017.2679006.
- [48] H. Ma, J. Gou, X. Wang, J. Ke, and S. Zeng, "Sparse Coefficient-Based k -Nearest Neighbor Classification," *IEEE Access*, vol. 5, pp. 16618-16634, 2017, doi: 10.1109/ACCESS.2017.2739807.
- [49] A. Swetapadma and A. Yadav, "A novel single-ended fault location scheme for parallel transmission lines using k -nearest neighbor algorithm," *Computers & Electrical Engineering*, vol. 69, pp. 41-53, 2018/07/01/ 2018, doi: 10.1016/j.compeleceng.2018.05.024.
- [50] W. Zhang, X. Chen, Y. Liu, and Q. Xi, "A Distributed Storage and Computation k -Nearest Neighbor Algorithm Based Cloud-Edge Computing for Cyber-Physical-Social Systems," *IEEE Access*, vol. 8, pp. 50118-50130, 2020, doi: 10.1109/ACCESS.2020.2974764.
- [51] C. Zhang, Q. Guo, and Y. Li, "Fault Detection in the Tennessee Eastman Benchmark Process Using Principal Component Difference Based on K -Nearest Neighbors," *IEEE Access*, vol. 8, pp. 49999-50009, 2020, doi: 10.1109/ACCESS.2020.2977421.
- [52] S. A. Boggs, "Partial discharge. II. Detection sensitivity," *IEEE Electrical Insulation Magazine*, vol. 6, no. 5, pp. 35-42, 1990, doi: 10.1109/57.63081.
- [53] G. C. Stone, "Partial discharge diagnostics and electrical equipment insulation condition assessment," *IEEE Transactions on Dielectrics and Electrical Insulation*, vol. 12, no. 5, pp. 891-904, 2005, doi: 10.1109/TDEI.2005.1522184.
- [54] T. Cover and P. Hart, "Nearest neighbor pattern classification," *IEEE Transactions on Information Theory*, vol. 13, no. 1, pp. 21-27, 1967, doi: 10.1109/TIT.1967.1053964.
- [55] C. Jing and J. Hou, "SVM and PCA based fault classification approaches for complicated industrial process," *Neurocomputing*, vol. 167, pp. 636-642, 2015/11/01/ 2015, doi: 10.1016/j.neucom.2015.03.082.

- [56] H. Guo and W. Wang, "An active learning-based SVM multi-class classification model," *Pattern Recognition*, vol. 48, no. 5, pp. 1577-1597, 2015/05/01/ 2015, doi: 10.1016/j.patcog.2014.12.009.
- [57] Y. Liu, Z. You, and L. Cao, "A novel and quick SVM-based multi-class classifier," *Pattern Recognition*, vol. 39, no. 11, pp. 2258-2264, 2006/11/01/ 2006, doi: 10.1016/j.patcog.2006.05.034.
- [58] M. Carrasco, J. López, and S. Maldonado, "A multi-class SVM approach based on the l_1 -norm minimization of the distances between the reduced convex hulls," *Pattern Recognition*, vol. 48, pp. 1598-1607, 12/17 2014, doi: 10.1016/j.patcog.2014.12.006.
- [59] A. A. Mazroua, M. M. A. Salama, and R. Bartnikas, "PD pattern recognition with neural networks using the multilayer perceptron technique," *IEEE Transactions on Electrical Insulation*, vol. 28, no. 6, pp. 1082-1089, 1993, doi: 10.1109/14.249382.
- [60] A. Costalago Meruelo, D. M. Simpson, S. M. Veres, and P. L. Newland, "Improved system identification using artificial neural networks and analysis of individual differences in responses of an identified neuron," *Neural Networks*, vol. 75, pp. 56-65, 2016/03/01/ 2016, doi: 10.1016/j.neunet.2015.12.002.
- [61] B. Boyle and T. p. Serdar, *Support Vector Machines: Data Analysis, Machine Learning and Applications*. 2011.
- [62] W. Jee Keen Raymond, H. A. Illias, and A. H. Abu Bakar, "Classification of Partial Discharge Measured under Different Levels of Noise Contamination," *PLOS ONE*, vol. 12, no. 1, p. e0170111, 2017, doi: 10.1371/journal.pone.0170111.